CLEARINGHOUSE FOR FEDERAL SCIENTIFIC AND TECHNICAL INFORMATION CFSTI
DOCUMENT MANAGEMENT BRANCH 410.11

LIMITATIONS IN REPRODUCTION QUALITY

ACCESSION # AD607517

☑ 1. WE REGRET THAT LEGIBILITY OF THIS DOCUMENT IS IN PART UNSATISFACTORY. REPRODUCTION HAS BEEN MADE FROM BEST AVAILABLE COPY.

☐ 2. A PORTION OF THE ORIGINAL DOCUMENT CONTAINS FINE DETAIL WHICH MAY MAKE READING OF PHOTOCOPY DIFFICULT.

☐ 3. THE ORIGINAL DOCUMENT CONTAINS COLOR, BUT DISTRIBUTION COPIES ARE AVAILABLE IN BLACK-AND-WHITE REPRODUCTION ONLY.

☐ 4. THE INITIAL DISTRIBUTION COPIES CONTAIN COLOR WHICH WILL BE SHOWN IN BLACK-AND-WHITE WHEN IT IS NECESSARY TO REPRINT.

☐ 5. LIMITED SUPPLY ON HAND: WHEN EXHAUSTED, DOCUMENT WILL BE AVAILABLE IN MICROFICHE ONLY.

☐ 6. LIMITED SUPPLY ON HAND: WHEN EXHAUSTED DOCUMENT WILL NOT BE AVAILABLE.

☐ 7. DOCUMENT IS AVAILABLE IN MICROFICHE ONLY.

☐ 8. DOCUMENT AVAILABLE ON LOAN FROM CFSTI (TT DOCUMENTS ONLY).

☐ 9.

PROCESSOR: CA

TSL-107-10 64

THE RAMO-WOOLDRIDGE CORPORATION
Guided Missile Research Division

EXPERIMENTS ON THE VIBRATION OF THIN CYLINDRICAL SHELLS UNDER INTERNAL PRESSURE

by

Y.C. Fung, A. Kaplan and E.E. Sechler

Report No. AM 5-9

15 December 1955

Aeromechanics Section

Approved M.V. Barton
M. V. Barton

CONTENTS

ILLUSTRATIONS

TABLES

SUMMARY

Experimental results on the frequency spectra, vibration modes, and structural damping of a series of thin-walled cylinders subjected to internal pressure are presented.

Within the estimated accuracy, the experimental results show good agreement with the features predicted by the linear theory of elastic shells.

SYMBOLS

p	internal pressure, pounds per square inch, gage
p_T	pressure in the tension control bellows, pounds per square inch, gage
m	number of longitudinal half-waves
f	frequency, cycles per second
amp	relative amplitude
N_x	tension in the axial direction of the shell, pounds per inch
N_ϕ	tension in circumferential direction of the shell, pounds per inch
ρ	density of shell material
h	wall thickness
L	length of cylinder

INTRODUCTION

Recent studies (Refs. 1-4) on the vibration of thin cylindrical shells under internal pressure show several rather surprising results:

1. The natural frequencies are arranged in an order which has little relation to the complexity of the nodal pattern.

2. At small values of internal pressure, the mode corresponding to the lowest frequency is very sensitive to the variation of internal pressure. The nodal pattern at the lowest frequency changes rapidly with the internal pressure.

3. Beginning with the unpressurized case, the lowest frequency first increases rapidly with increasing internal pressure, then the rate of increase slows down until ultimately it varies with the square root of the internal pressure.

In order to verify these results, experiments were performed on models available at the time. Frequency data were obtained which give good correlation with the theory; but, owing to the small size of the models, only the simpler vibration modes could be determined with certainty. Those determined, however, did agree with the theoretical predictions. An effort was made also to determine the damping characteristics of the model.

SECTION I
APPARATUS AND PROCEDURES

TEST SPECIMENS

The models used for the tests (see Fig. 1) were cylinders with a 3.5-inch inside diameter, made of 24S-H aluminum alloy sheets (condenser foil) of three thicknesses--0.001, 0.002, and 0.003 inches, and three axial lengths--11, 7, and 3.5 inches. The material was furnished by Alcoa, and the cylinders were made by the Task Corporation, Pasadena. The cylinders were made by cementing the sheets together with lap joints in the axial direction. The two ends were cemented to rings which provided a seal for internal pressure.

The end rings were made of brass and were much heavier than the cylinders, thus ensuring circular cross sections at the ends. The end rings were free to move longitudinally and, to a certain degree, were free to rotate as a rigid body.

Figure 1 shows the test specimen, the pressurization system, and the vibration pick-up buttons. The front end of the cylinder was sealed by a solid nose. The end rings of the test specimen rested on a 2-inch-diameter central shaft which had holes conveying the controlled internal pressure into the cylinder. Nitrogen bottles were used as a pressure source. It was possible to control the internal pressure to within limits of ± 0.01 psi.

At the rear end of the test specimen, the end ring was fastened to a floating ring which was sealed against the shaft by a flexible bellows. To this floating ring were attached four bellows which were capable of exerting a longitudinal compressive load on the cylinder, and two bellows capable of exerting a tensile load on the cylinder. By controlling the pressures in these bellows, the axial stress in the cylindrical shell was controlled over a very wide range.

TEST SETUP

Figure 2 shows a schematic diagram of the test setup. The motion of the cylinder was excited by a sound generator through a loud speaker. The

output from the speaker was so adjusted as to maintain a constant sound level of 70 db at a microphone situated about 2 ft from the cylinder. The speaker was placed about 2 ft on the opposite side of the cylinder. (Changing the speaker location and direction did not seem to have any significant effect on the frequence response.) During a resonant oscillation, the cylinder itself generated a considerable amount of sound. It would be desirable to maintain a constant level of the excitation; but this was not possible because the sound intensity from the sound generator and speaker was not a smooth function of frequency but was rather erratic. Since only the resultant of the sound generated by the speaker and the cylinder was kept constant, the excitation near the resonance condition was less than 70 db. In other words, the resonance peak in the frequency response curves of the cylinder oscillation were artificially reduced in amplitude. This fact must be remembered in interpreting the relative amplitude data presented later.

It was possible to maintain a 70-db sound level between approximately 100 to 8000 cps. Beyond 8000 cps, the output from the speaker dropped sharply. The natural frequencies of the cylinder were recognized through resonance.

The motion of the cylinder was measured by the variation of the gap between the cylinder and a number of brass buttons which rested on an inner tube of polysteyrene. The cylinder and the buttons were charged and formed individual condensers, the variation in capacitance of which was measured. The gap between the cylinder and the button was nominally 0.040 in. under no-load condition; however, this spacing could not be controlled very accurately. Only the relative variations in output of a given button were of significance, whereas the absolute values of the output by various buttons must not be regarded as too significant.

It was necessary to insert vacuum tubes right next to the brass buttons inside the cylinder; hence, in a continued run, the cylinder became quite hot to the touch.

Buttons 1 through 13 were of 1/2- by 1/2-inch cross section; buttons 14 through 24 were of 1/8- by 1/8-inch cross section. Figure 3 shows the numbering of the buttons. For the 11-inch models, there were 24 buttons, with 10 buttons equally spaced along an axial line and two circles of 8 buttons each uniformly spaced. For the 7-inch models, only buttons 1-12 were used; for the 3.5-inch models, only buttons 2-11.

Figure 2 also shows the pressurization system. The internal pressure was checked by manometer and, much more sensitively, by a Honeywell-Brown read-out device which had been calibrated by a mercury micromanometer.

INSTRUMENTATION

Figure 4 shows schematically the instrumentation used in measuring the signal from the pick-up buttons. A selector switch was used because the instruments could read the signal from only one button at a time. After passing through an amplifier, the signal was observed in three ways:

1. Oscilloscope. This showed the wave form, relative amplitude, and Lissajou curves between signals coming from any two buttons. Lissajou curves were recorded photographically by a Polaroid-Land camera, and were used to identify the vibration modes. In the last mentioned function, one button, usually No. 3, was selected as a reference and Lissajou curves with respect to the other buttons were recorded.

2. Harmonic Wave Analyzer. A Model 300A Harmonic Wave Analyzer, made by the Hewlett-Packard Co., Palo Alto, Calif., was used. It was a selective voltmeter, covering the audio spectrum from 30 to 16,000 cps. It had a voltage range from 1 mv to 500 volts, with an over-all voltage accuracy of $\pm 5\%$. Selectivity was so set that when the deviation from the center frequency was 30 cps there was a drop of 40 db in response. Frequency was read from a Berkeley Universal Counter and Timer, Model 5510. This counter could also be connected to the sound generator to read the frequency of the forcing function.

3. Voltmeter. The signal could also be read directly from a voltmeter. It was found that a direct correlation existed between the voltmeter readings and the harmonic wave analyzer readings. Hence, whenever it was ascertained that the cylinder vibration frequency agreed with the speaker frequency, the relative amplitude of the cylinder motion was read from the voltmeter.

With respect to the measurement of phase relationship between the signals from the various buttons, a Type 405 Precision Phase Meter, made by the Advance Electronics Co., Passaic, N. J., was used at the beginning; however, its use was so time-consuming that it was discontinued later.

TEST PROCEDURE

Each series of tests began with the unpressurized case. The frequency spectrum was first determined, the phase relationship and mode shapes were then studied, and from time to time the damping characteristics were recorded. In several cases of the unpressurized cylinder, measurements on the frequency and damping were made both with and without the nose seal. No significant difference was discovered. Spot checks were made also on the effect of the longitudinal tension control bellows on the frequency and damping; when these bellows are unpressurized they should have little effect on the vibration of the cylinder. Experiments did show that neither the frequency nor the damping was appreciably affected by inserting or removing the bellows. Details of the measurements are described below.

Frequency Spectrum

During each run an internal pressure was selected and maintained constant. The sound generator was then tuned to give a 70-db sound at a low frequency. This frequency was measured by the Berkeley counter. When this exciting frequency was varied, the output from the pick-up buttons varied. In most cases it was quite easy to pick out a resonance peak either on the oscilloscope or on the voltmeter. But there were cases in which large responses occurred over a fairly wide band of frequencies, and it was somewhat difficult to decide which were the natural frequencies. Occasionally, beating occurred, as could be seen on the oscilloscope. There were also cases in

which the wave form appeared complicated. These difficulties were disturbing at first sight, but after some reflection it appeared to be just what should be expected, because of the general behavior of a cylinder and of the effect of slight degrees of asymmetry that existed in the model. More detailed discussion will follow in a later section.

Mode Shape

At a resonance condition, the amplitude and phase of the signal from various buttons (with respect to button 3) were determined one by one. These were then plotted (see Fig. 12) to show the instantaneous geometrical relations. For simpler modes, it was possible to ascertain the mode shape. The determination was limited only by the number of pick-up buttons. Examples of Lissajou curves are shown in Figure 12. The signal from button 3 was chosen as the x-component, and that from the other buttons as the y-component. Plotting in the same way as before determined the mode shape whenever permissible.

Damping Characteristics

The sharpness of the sound generator, the sharpness of the cylinder response signal, and the frequency response curve near resonance were measured. The inference of damping characteristics will be discussed later.

SECTION II
TEST RESULTS

FREQUENCY

Tables 1 through 8 show the frequency spectra recorded. In these tables, "f" denotes frequency in cycles per second, "amp" denotes relative amplitude in millivolts read from the voltmeter or harmonic analyzer, and "p" is the internal pressure in psig, i.e., the pressure differential across the shell.

The model designation 11-001 indicates that the axial length of the model was 11 inches and that the wall thickness was 0.001 inch. Similarly, 3.5-002 means a length of 3.5 inches and a wall thickness of 0.002 inch.

All tables, unless specifically mentioned, refer to models in which the axial-tension and compression control bellows were removed. The frequencies so observed are plotted as small circles in Figures 5-10.

Some footnotes must be added. In model 11-001, a large response at a frequency of 175 cps was observed at all values of pressure p, and a smaller response at a frequency of 555 cps was present at all values of p greater than 0.2. These responses were identified by the mode-shape determinations from the Lissajou curves as the first and second rigid-body modes (m = 1, 2; n = 1); they belong to a different category of vibration in which the inertia of the masses attached to the ends of the cylinder becomes of importance, hence they are not listed in Table 1.

In the model 11-002, a small response at a frequency of 172 cps was observed at p = 0 and 0.10 psig; at a frequency of 760 cps, a large response was observed at p = 1.0, whereas, rather small responses were observed at p = 2.0, 3.0, and 4.95 psig. Although no examination of these mode shapes was made, it was assumed that they also corresponded to the first and second rigid-body modes, therefore, these frequencies have been omitted from Table 2. In Tables 3-8, all of the observed frequencies were recorded.

Figure 11 shows a continuous plot of the frequency response of cylinder 001 at a nominal pressure of 0.50 psig, with the axial-tension control

bellows inserted, to the sound excitation whose resultant output was 70 db. There were areas in which the response was very large over a wide range of frequencies. These occurred when there were several natural frequencies in the same neighborhood. This figure is a simplification of the actual picture which contains many more little peaks and valleys in the frequency response curves. In taking the readings for Tables 1-8, these small bumps were neglected, except in Table 7, which was taken in greater detail.

Table 3 for model 11-003 and Table 6 for model 3.5-001 are briefer than the others. Only the most obvious resonances were recorded in these tables. The data in Table 8 refer to a model 11-001 in which the axial-tension control bellows were inserted and pressurized. This particular set of data and also those of Figure 11, however, were taken when nitrogen bottles as the source of pressure were not available, and the laboratory air line was connected to pressurize the cylinder. The control of pressure was very difficult under this condition, and it fluctuated beyond control. The data, therefore, can serve only to show trends in which the p-readings were merely nominal.

The following information is needed for interpretation of the data in Table 8. The net area of the tension bellows was 0.52 sq in., and the membrane tension in the axial direction induced in the cylinder wall was therefore

$$N_x = \frac{0.52\ p_T}{3.5\ \pi} = 0.0472\ p_T,\ \text{lb per inch},$$

where p_T is the pressure in the bellows in psig. This should be added to the membrane tension caused by the internal pressure

$$N_x = \frac{pa}{2}\ \frac{\text{effective free end area}}{\text{cylinder cross section}}$$

$$= \frac{pa}{2}\ \frac{6.06\ \text{inch}^2}{9.61\ \text{inch}^2}$$

$$= 0.552\ p,\ \text{lb per inch}$$

$$= 0.315\ N_\phi.$$

The theoretical correction to frequency due to the pressure in the tension bellows can be expressed most concisely in terms of the change in the square of the frequency, Δf^2, where f is in cycles per second,

$$\Delta f^2 = \frac{m^2 N_x}{4 \rho h L^2} = 377\, m^2\, p_T ,$$

m is the number of axial half-waves, and p_T is in psig. By comparing the figures in Table 1, it can be seen that the theoretical corrections are not large.

Each spectrum in these tables terminated at a reading beyond which the response signals were rather small, under which condition the determination of resonance became dubious.

Table 4 gives an illustration of an unsuccessful way of determining the lowest frequency, and it also shows a peculiar characteristic of cylinder vibration. In this test, the lowest frequency was determined at p = 0. The pressure was then increased in small steps, while the frequency was varied in small increments in such a way that a large response was held on the oscilloscope. It was thought that the lowest frequency, as a function of internal pressure, could thus be traced. These points were plotted in Figure 7 as a circle with a dagger. It was apparent that the frequency-pressure trace did not follow a single mode-shape line, but that it shifted to another mode as the operation proceeded without any obvious warning.

MODE SHAPE

Vibration mode studies were concentrated on the 11-inch models. Altogether more than 40 modes were identified for the 11-001 model. Figure 12 shows a few examples of the approximate determination of the vibration modes. The film recorded the Lissajou curves, from various buttons successively. The x-component was from button 13. The y-component was from other buttons arranged in the following manner:

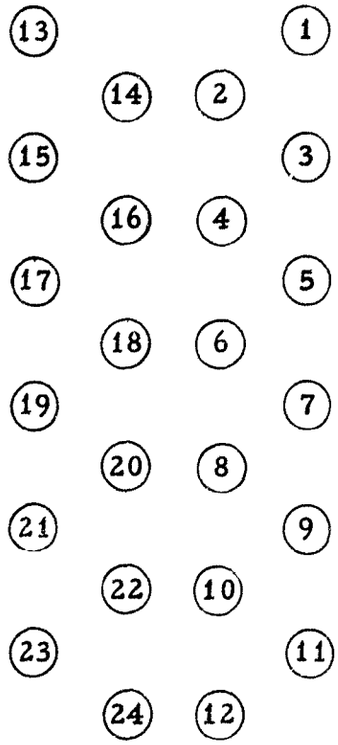

A line in the second quadrant means in phase with button 3; that in the first quadrant means out of phase. The circuit for button 8 was open during the recording, hence the trace for that button appeared as a horizontal line. The attenuation for buttons 14-24 was 10 times smaller than that used for buttons 1-13.

As mentioned previously, the nominal distance of 0.040 inch between the shell and the buttons was not controlled. Hence the accuracy of the relative amplitude was not high and has only a qualitative significance.

Several examples of the Lissajou curves are shown in Figure 12 together with the mode shapes which were determined from them.

Results obtained from the harmonic analyzer, voltmeter, and the phase meter agreed well with the Lissajou curve determinations. For conciseness these data are not presented here.

Because of the complicated mode shapes (large n) for very thin cylinders at low pressure ($p = 0$, or 0.05 psi), the determination of the modes

was difficult with the relatively small number (24) of sensing elements used. At higher internal pressure, however, the modes corresponding to the lower frequencies were readily recognized.

All modes identified agreed with the theoretical predictions.

DAMPING

The sharpness of the frequency output of the sound generator, at specific settings, was measured. Some typical curves, chosen for several frequencies ranging from 500-4000 cycles per second are shown in Figure 13. The amplitude scale was arbitrarily chosen so that these curves appear to be more or less of the same height.

The sharpness of the response of the cylinder at a specific forcing frequency is shown in Figure 14. The frequency response, ie . the variation of peak response values with the forcing frequencies, is illustrated in Figure 15.

The most striking features of all the curves shown in Figures 13-15 is that the half-band width in frequency did not seem to vary much with frequency range and internal pressure; nor did it vary much with insertion or removal of the axial-tension-control bellows. The results from the harmonic analyzer and the voltmeter appeared similar, although there were some differences in the details. These differences were well within the experimental accuracy and cannot be analyzed with certainty.

To interpret the above result, an analysis was made (see appendix) of the expected half-band width as a function of the sharpness of the forcing function, the damping characteristics (transfer function) of the cylinder, and the resonance characteristics of the harmonic analyzer. It is concluded that the half-band width of the transfer function is about equal to that of the harmonic analyzer The structural damping coefficient, g, as ordinarily used in flutter analysis, does not remain constant; instead the product gf, does remain nearly constant for a wide range of frequencies. The experimental results may be summarized as

$$gf = 6 \text{ cycles.}$$

where f is the frequency in cycles per second. Since gf is ordinarily identified as the viscous damping coefficient, one may say that the damping characteristics of the model were of a viscous nature. More precisely, if ϕ_n represents the n^{th} normal mode of the cylinder, the Lagrange equation of motion for free oscillation may be written in the form

$$\ddot{\phi}_n + c_n \dot{\phi}_n + \omega_n^2 \phi_n = 0, \qquad (c_n \doteq 2\pi f_n g)$$

where ω_n is the natural frequency corresponding to ϕ_n. Our experimental results seem to show that c_n is a constant for all values of n.

SECTION III
DISCUSSION

ACCURACY OF THE EXPERIMENTAL RESULTS

The uncertainties of the experimental results came mainly from the pressure control. In most runs (each spectrum required about two hours) the internal pressure fluctuated within limits of ± 0.01 psig. In a few cases a variation of ± 0.02 psig was tolerated. The latter cases occurred on days of very hot weather during which control of the pressure appeared to be more difficult; these cases are readily reflected in the shortness of the spectra in Tables 1-8. (Fewer data were taken under these conditions.)

Determination of the resonance condition was difficult when there were several natural frequencies crowded together or even coincident. The difficulty was further accentuated by the resolution of a single theoretical natural frequency into two because of the small asymmetries of the models (the contribution of the seams and other geometric and dynamic irregularities). Examples can be seen in Figures 15(a), (f) and (n). Generally the small peaks in the neighborhood of a large resonance peak were not recorded.

Repeated tests on different days of testing for nominally the same test conditions revealed that an uncertainty of approximately 1% in frequency should be allowed.

THEORETICAL RESULTS

Theoretically the vibration modes of the cylindrical shells can be identified by the nodal lines of the radial displacements. A pair of integers, (m, n), specifies a mode in which there were m longitudinal half-waves and n circumferential waves or 2n circumferential nodes. The nodal lines for radial displacements are not lines of absolute rest for tangential displacements take place along these lines. Accordingly there are three frequencies associated with each vibration pattern. The lowest

frequency is associated with the mode with predominantly radial motion. The two higher frequencies are associated with the same radial pattern, but with larger circumferential and longitudinal displacements. The higher frequencies are at least about 20 times higher than that of the predominately radial mode for cylinders whose geometrical dimensions approach those of the test models.

Curves of frequency vs. internal pressure for each nodal pattern cross and recross each other. Curves of frequency at a given internal pressure for various axial wave lengths also cross and recross each other. As a result, the frequency spectrum appears highly irregular. Several modes may have the same or nearly the same frequency. Beating at a certain frequency range is, therefore, to be expected.

The theoretical results for "freely supported" cylinders are plotted in Figures 5-10. The solid curves refer to $m = 1$, the dotted curves to $m = 2$, and the chain dots to $m = 3$. Frequencies for $m > 3$ are not plotted here. The bending modes, $n = 1$, are also omitted from these plots, since in these modes the masses attached to the ends of the cylinder contribute significantly to the frequencies; whereas, for $n \geq 2$, the end masses, if rigidly connected, are of small influence. The theoretical curves in Figures 5-11 are based on Reissner's results (Ref. 3). A comparison of Reissner's approximate expression with the more complicated and exact results (Ref. 4) shows that the error is small for large n, but for $n = 2$ an error of the order of 5 to 10% might be expected, the exact error being dependent upon the ratio of the radius to the axial wave lentgh. All of the approximate frequencies are higher than the exact theoretical values.

The theoretical curves in these figures are computed for freely supported ends. The actual end conditions of the test specimens were somewhere between freely supported and clamped. Reference 2 shows that, for an unpressurized cylinder, $p = 0$, the frequencies for the clamped ends are higher than those for the freely supported ends, and these frequencies can be estimated approximately by replacing m by $(m + c)$ in the formula for the freely supported ends. The constant, c, lies between 0.2 to 0.4. The theoretical effect of the end conditions on frequency in the pressurized

case has not yet been determined. It seems evident that the theoretical values for the frequencies of the test specimens should be higher than the freely supported curves shown in Figures 5-11, the error being largest for m = 1. On the other hand, the apparent mass of air was neglected in the theoretical curves. If it were included, the frequencies would be lowered. These factors of opposing influences have not yet been evaluated theoretically.

Tobias, in Reference 5, shows that the effect of small asymmetries in the cylinder is to resolve a single natural frequency into two nearby values. If a given steel cylinder, which in engineering practice is always dynamically unsymmetrical, is excited by a small electromagnetic excitor, the peak does not necessarily occur under the excitor. When the excitor is rotated around a circumference of the cylinder, two locations, usually 90 degrees apart, can be determined at which the amplitude is the largest and at which one single peak at resonance is observed at each of these locations. The frequencies at these two locations are more or less different, depending on the degree of deviations from dynamic symmetry. For an excitor located at any other position, two peaks appear in the frequency response curve, usually one larger than the other. If the asymmetry is large, these peaks move sufficiently apart to appear as two distinct peaks.

The phenomenon referred to by Tobias makes an experimental determination of the natural frequency by resonance somewhat difficult. Some of the extraneous frequencies that appear in Figures 5-10 are undoubtedly due to this origin.

AGREEMENT BETWEEN THEORY AND EXPERIMENT

The experimental results certainly showed all the important features predicted by the theory. In examining the numerical agreement, it should be remembered that an error of $\pm 1\%$ in observed frequency and a variation of ± 0.01 psi in internal pressure (for shorter spectra, a variation of ± 0.02 psi) should be allowed. The discrepancy between the

theory and experiment arises from several sources. The most important is probably the end conditions. So far only the freely supported ends have been studied theoretically for the pressurized cylinder. It seems worthwhile to evaluate the theoretical effects of other end conditions. The error caused by the shallow-shell approximation could be removed on the basis of existing theory, but the laborious computation was not attempted in writing this report. The dynamic asymmetry is probably responsible for some of the extraneous points recorded on Figures 5-10, also for some of the deviations between the experimental and theoretical values. Some of the other experimental points that do not fall on any theoretical curves may perhaps be explained by higher values of m because curves for $m > 3$ are not plotted in these figures. Curves for $m > 3$ would appear at higher frequencies. Thus, in Figure 10, the left upper corner would have been covered by curves of this category.

The simpler vibration modes that can be identified with the test equipment all agree with the theoretical predictions.

SECTION IV
CONCLUSIONS

It appears from the foregoing that the experiments and the theory, as presented in References 1-4, are in reasonable agreement. For cylinders with freely supported ends, Reissner's approximate frequency expression is adequate for prediction at high internal pressures for all values of n, and at lower internal pressures for $n \geq 3$. The effect of other end conditions on the frequency should be a worthwhile subject for further research.

The experiments reveal the complicated nature of cylinder vibration and point to various difficulties in obtaining accurate data. Without a theoretical background, it is virtually impossible to understand the mass of frequency readings. Furthermore, whether a mode will be strongly excited or not in a resonance test depends entirely on the method of excitation; consequently, important modes may be overlooked in a specific experimental arrangement. This points to the extraordinary importance of theoretical calculations in the cylinder vibration problem. On the other hand, the experimental results presented in this report show clearly that the magnitude of the response has no simple relation to the order of the frequency in the spectrum. Thus a very large response may occur at a frequency which is several times the lowest one and which is of a large order in the spectrum. Hence, in engineering applications of the cylinder vibration theory, it is imperative that the calculations be not stopped at the first few lowest frequencies, but that the whole spectrum in the frequency range of interest be examined.

Table 1. Frequency Spectra, Model 11-001.

p = 0		p = 0.05		p = 0.10		p = 0.20		p = 0.50		p = 1.00		p = 2.00		p = 3.50		p = 4.95	
f	amp	f	amp	f	amp	f	amp	f	amp	f	amp	f	amp	f	amp	f	amp
216	280	354	22	465	80	534	18	756	74	872	10	1114	42	1167	34	1189	12
247	150	392	30	528	120	566	10	1080	88	987	10	1713	8	1433	14	1239	10
277	175	519	22	577	80	827	11	1134	40	1134	10	1845	12	1758	8	1663	16
314	230	587	24	673	80	853	16	1231	32	1210	10	2067	28	1883	18	2176	10
337	100	600	20	687	30	937	22	1386	85	1340	22	2375	28	2250	18	2610	32
355	30	635	12	732	16	1068	55	1430	20	1520	8	2760	18	2436	24	3116	18
379	80	681	14	863	30	1122	70	1470	34	1697	34	2886	44	2769	18	3156	60
445	45	733	14	885	28	1143	60	1552	26	1823	24	3207	22	3018	24	3174	30
454	50	760	20	907	32	1188	42	1669	28	2042	80	3444	48	3251	22	3457	30
549	100	816	14	925	36	1276	50	1676	98	2165	30	3598	20	3560	28	3639	44
578	30	841	28	941	36	1344	42	1768	35	2673	20	4013	55	3819	70	3709	45
604	20	931	42	959	28	1408	50	1934	32	2739	44	4223	32	3937	50	3992	35
660	20	944	24	1059	88	1488	60	2118	32	2949	16	4367	45	4030	70	4188	75
712	15	954	38	1073	28	1583	25	2256	40	3029	34	4747	28	4383	46	4602	12
1019	20	985	28	1092	150	1713	60	2283	38	3178	24			4624	28	4735	18
1132	30	999	72	1138	100	1794	40	3373	52	3511	64			5360	44	5323	8
1170	30	1040	90	1158	60	1983	42	3805	18	4225	40						
1727	20	1051	145	1177	30	2162	185	4466	22								
1771	20	1076	80	1261	25	2238	58	4658	40								
		1100	65	1356	60	2308	40										
		1165	85	1465	45	3077	30										
		1185	48	1480	20	5145	20										
		1218	65	1517	20	5372	32										
		1260	30														
		1330	46														
		1343	80														
		1450	48														

p = internal pressure, psig
f = frequency, cps
amp = relative amplitude, reading from voltmeter, mv

Note: A large response at f = 175 was observed at all values of p. A smaller response at f = 555 was present at all values of p greater than 0.20. These responses were identified as the first and second rigid-body modes (m = 1, 2; n = 1) (see Fig. 12a)

Table 2. Frequency Spectra, Model [illegible]-002.

p = 0		p = 0.10		p = 0.20		p = 0.50		p = 1.00		p = 2.00		p = 3.00		p = 4.95	
f	amp	f	amp	f	amp	f	amp	f	amp	f	amp	f	amp	f	amp
318	100	420	90	500	23	639	16	763	90	941	33	1040	41	1171	28
498	95	488	6	511	10	662	28	822	74	948	30	1115	71	1274	40
517	35	550	62	525	31	818	65	1014	29	1107	62	1573	90	1667	80
537	42	645	7	570	11	855	11	1106	120	1280	58	1607	12	1830	41
566	58	662	48	615	19	950	44	1134	28	1387	28	1696	32	2011	14
623	120	696	24	681	8	961	22	1156	46	1423	70	1876	68	2096	20
659	80	713	30	700	13	1027	19	1208	160	1552	18	2429	24	2114	19
690	30	817	22	740	43	1048	23	1340	85	1558	14	2464	10	2141	8
710	31	911	20	774	20	1149	130	1544	15	1646	40	2490	25	2333	7
736	18	950	16	796	32	1197	35	1696	50	1759	10	2654	38	2393	20
767	22	975	10	919	20	1211	42	1713	50	1795	15	2918	30	2434	8
867	8	1027	12	933	11	1276	25	1733	77	1840	22	3183	11	2568	15
895	8	1064	30	941	10	1301	30	1894	10	1920	48	3320	8	2785	21
1040	10	1072	35	999	10	1314	25	1958	14	2057	30	3504	15	3029	11
1086	22	1080	26	1042	14	1444	62	2075	9	2282	25	3754	10	3437	9
1139	100	1103	17	1074	23	1456	24	2121	17	2439	12	3906	15	3524	11
1227	50	1129	70	1102	50	1491	13	2472	42	2591	25	4571	8		
1598	15	1162	120	1199	110	1590	22	2866	16	2709	5				
1861	15	1244	40	1304	22	1697	20	4865	25	2842	10				
		1290	18	1396	10	1715	14			2894	13				
		1317	13	1425	9	1768	17			3479	13				
		1328	35	1458	7	1799	25			3650	10				
		1401	18	1500	11	1866	16			3763	17				
		1468	12	1553	11	1945	11			5352	5				
		1483	6	1755	25	1970	24								
		1586	8	1814	14	1998	10								
		1754	16	1849	21	2060	5								
		1801	19	1901	11	2191	5								
		1888	26	2363	8	2396	8								
		2320	10												
		2421	7												
		2437	11												

Table 3. Frequency Spectra, Model 11-003.

p = 0.00	p = 0.10	p = 0.50	p = 0.99	p = 1.48	p = 2.00	p = 2.72
387	440	583	736	776	849	931
453	452	666	854	857	910	957
563	529	788	1041	883	965	1098
631	542	1108	1108	1008	1144	1176
660	648	1182	1182	1173	1194	1207
725	697			1200		
757	764					
784	852					
864	1031					
951	1382					
1054	1398					
	1604					
	1678					
	1968					
	2211					
	2398					
	3854					

p = 2.98	p = 3.22	p = 3.51	p = 3.96	p = 4.50	p = 4.95	
954	968	988	1014	1040	1054	
984	1006	1198	1083	1240	1176	
1142	1212	1232	1212	1611	1217	
	1420	1478	1503			
		1552	1564			

No amplitudes were measured.

Table 4. Variation of the Lowest Frequency with Pressure.

p	f	p	f
0.0	387	2.72	931
0.1	440	2.98	954
0.21	491	3.22	968
0.30	527	3.51	988
0.40	560	3.96	1014
0.50	583	4.50	1040
0.85	680	4.95	1054
0.99	703		
1.15	729		
1.33	757		
1.48	776		
2.00	849		

Table 5. Frequency Spectra, Model 7-001.

p = 0		p = 0.10		p = 0.20		p = 0.30		p = 0.50		p = 1.0	
f	amp	f	amp	f	amp	f	amp	f	amp	f	amp
376	110	609	15	775	18	834	15	961	7	1194	20
412	90	648	40	1013	40	966	10	1223	42	1258	40
429	80	707	60	1435	40	1063	20	1375	120	1435	40
462	75	841	25	1467	25	1206	30	1468	46	1450	29
552	150	1225	25	1541	35	1257	15	1525	75	1634	175
594	60	1281	17	1616	28	1358	15	1751	90	1646	40
622	60	1321	27	1723	35	1439	40	1844	76	1900	50
646	70	1437	33	1940	10	1491	30	1875	25	2096	170
661	115	1510	14			1523	10	4042	15	2269	40
674	65	1615	17			1626	50			2386	80
706	25	1782	50			1670	15			2487	25
715	20	1900	35			1694	30			2524	25
727	33	1958	20			1773	60			2634	30
750	42					1836	36			3136	25
812	15									3197	30
833	35									3894	40
913	20									4510	100
967	13									4839	60
1620	40									5472	25
2379	7										

p = 2.00		p = 2.89		p = 3.50		p = 3.92		p = 4.95	
f	amp	f	amp	f	amp	f	amp	f	amp
1395	250	1532	50	1653	190	1698	85	1818	500
1488	360	1614	72	1777	35	1937	60	2159	210
1567	70	1712	120	1872	520			2586	30
1719	90	5356	3	2212	260			3066	60
2017	90			2235	20			3316	30
2289	40			2602	70			3390	28
2306	20			2999	50			3873	120
2598	50			3244	70			4033	80
2654	40			3446	50			4479	60
2902	85			3863	70			4569	50
3248	90			4286	140			4732	38
3652	95			4410	25			4954	70
3676	200			4502	40			5015	140
3996	70			4775	130			5167	60
4809	200			4830	60			5207	45
5847	40			5235	60			5304	25
				7631	35			6183	50
								7559	20
								7889	10
								8637	10

Table 6. Frequency Spectra, Model 3.5-001.

p = 0.50		p = 1.00		p = 3.00		p = 4.95		p = 10		p = 13		p = 16	
f	amp	f	amp	f	amp	f	amp	f	amp	f	amp	f	amp
1477	40	1776	80	2402	210	2961	100	2580	70	2598	40	2570	45
1538	20	2136	20	2668	85	3308	30	2928	40	2912	30	2904	30
1898	19	2374	20	2982	80	3707	35	3127	170	3255	220	3372	120
2474	100	2539	90	3651	25	4136	75	3302	50	3616	70	3875	120
2622	30	2625	115	4054	30	5136	25	3840	45	4195	130	4575	80
2800	50	3044	60	4400	170			4433	150	4886	40	5957	20
2849	25	3282	80	4816	25			5735	35	5619	25	7965	30
5735	20			5941	60			6198	10				

Table 7. Frequency Spectra, Model 3.5-002.

p = 0		p = 0.05		p = 0.10		p = 0.20		p = 0.30	
f	amp	f	amp	f	amp	f	amp	f	amp
924	22	945	80	1047	75	1166	120	1248	130
959	21	1032	340	1099	560	1196	300	1270	80
1012	580	1044	160	1120	150	1244	50	1303	200
1077	280	1136	240	1216	400	1301	40	1316	110
1167	20	1219	240	1302	50	1433	350	1454	110
1410	34	1256	70	1368	350	1485	70	1633	30
1493	16	1373	130	1437	135	1539	90	1716	100
1667	16	1419	90	1615	45	1635	75	1790	40
1720	16	1626	50	1720	60	1740	60	2101	80
2060	10	1671	125	2188	100	2019	40	2226	90
2141	10	1696	40	2216	45	2136	30	2352	110
2310	140	1764	90	2280	60	2181	80	2446	30
2325	90	1898	30	2376	110	2194	40	2541	160
2365	110	1924	30	2456	30	2365	60	2614	40
2385	140	2087	25	2516	30	2398	260	2696	30
2481	200	2131	50	2546	75	2469	60	2731	50
2547	180	2277	50	2609	60	2525	20	2781	150
2614	80	2352	125	2661	140	2672	200	2824	250
2670	60	2394	80	2769	240	2728	80	2844	220
2749	160	2463	50	2835	240	2773	100	2877	280
2773	170	2527	170	2898	310	2853	280	3053	50
2823	85	2550	150	2955	70	2943	110	3130	30
2930	60	2622	90	3149	70	3008	40	3309	50
3189	70	2670	200	3397	40	3113	30	3399	30
3282	30	2699	50	3894	40	3324	90	3817	30
3423	70	2783	180	4210	110	4259	85	4041	70
3506	100	2834	280	4509	50	5135	45	4235	70
3572	80	2869	20	4623	40	5534	40	4470	60
3710	60	2949	70	4757	50	5672	25	4659	70
3866	35	3046	40	5037	50			4773	40
4214	20	3207	100	5577	40			4969	110
4419	20	3257	110					5116	40
4551	22	3513	90						
4607	62	3735	30						
4738	25	3828	30						
4847	50	4051	50						
5742	22	4170	25						
6897	22	4283	90						
		4460	40						
		4672	40						
		4953	40						
		5136	40						
		5434	40						

Table 7. Frequency Spectra, Model 3.5-002 (Cont'd).

p = 0.5		p = 1.00		p = 3.00		p = 4.95		p = 10.0	
f	amp	f	amp	f	amp	f	amp	f	amp
1396	150	1661	420	2215	170	2538	260	2712	64
1467	30	1830	40	2405	290	2942	300	3028	240
1540	80	2277	200	2438	70	3054	110	3179	130
1581	80	2325	250	2626	50	3266	210	3289	60
1767	105	2616	50	2847	200	3603	30	3621	120
1794	40	2783	115	2972	260	5115	40	4004	140
1864	35	2886	190	3124	100			4047	40
2065	30	3046	20	4037	90			4472	240
2253	25	3202	40	4102	100			4520	160
2456	30	3239	200	4129	30			4556	20
2538	20	3326	150	4167	30			5500	140
2644	95	3476	20	4378	90				
2768	100	4284	40						
2816	130	4830	30						
2845	150	5164	45						
2914	320								
2960	125								
3062	50								
3112	20								
3208	35								
3149	30								
3208	32								
3252	50								
3493	110								
3571	40								
3692	35								
4225	160								
4511	20								
4821	20								
5004	20								
5170	20								
5657	20								

Table 8. Frequency Spectra of Model 11-001 with All Six Axial-Tension Control Bellows Inserted and Operating.

p = 0 p_T = 30		p = 0 p_T = 60		p = 1.0 p_T = 60	
f	amp	f	amp	f	amp
301	30	246	60	874	6
386	30	305	80	969	15
422	20	350	40	1044	20
434	20	380	20	1194	50
537	25	400	20	1233	20
617	10	439	30	1291	40
699	40	577	10	1330	110
778	30	607	10	1423	20
800	20	663	20	1521	100
1159	20	701	25	1729	6
1517	6	831	20	2123	15
1606	6	905	10	2366	8
2919	8	1164	10	2556	6
		1553	10	2947	5
		2335	10		

APPENDIX

INTERPRETATION OF THE DAMPING MEASUREMENTS

Measurement of a Forcing Function by the Harmonic Analyzer

Let the forcing function be described by the bell-shaped curve

$$A \exp\left[-\frac{(\omega - \omega_1)^2}{2\lambda}\right], \tag{1}$$

where A and λ are constants and ω_1 is the peak frequency. Let the response characteristic of the harmonic analyzer be described by

$$B \exp\left[-\frac{(\omega - \omega_2)^2}{2\mu}\right], \tag{2}$$

where B and μ are constants and ω_2 is the frequency to which the analyzer is tuned. The reading of the analyzer is therefore approximated by the integral

$$F_1(\omega_2 - \omega_1) = A\,B\int_{-\infty}^{\infty} \exp\left[-\frac{(\omega - \omega_1)^2}{2\lambda}\right] \exp\left[-\frac{(\omega - \omega_2)^2}{2\mu}\right] d\omega. \tag{3}$$

Letting $x = \omega - \omega_1$ and $a = \omega_2 - \omega_1$, then the above integral becomes

$$F_1(a) = A\,B\int_{-\infty}^{\infty} \exp\left[-\frac{x^2}{2\lambda} - \frac{(x-a)^2}{2\mu}\right] d\omega$$

$$= A\,B\int_{-\infty}^{\infty} \exp\left[-\frac{1}{2}\left(\frac{1}{\lambda} + \frac{1}{\mu}\right) y^2 - \frac{a^2}{2\mu}\left(1 - \frac{\lambda}{\lambda + \mu}\right)\right] dy$$

$$= A\,B \exp\left[-\frac{a^2}{2(\lambda + \mu)}\right]\int_{-\infty}^{\infty} \exp\left[-\frac{1}{2}\left(\frac{1}{\lambda} + \frac{1}{\mu}\right) y^2\right] dy,$$

where

$$y = x - \frac{a\lambda}{\lambda + \mu} = \omega - \frac{\mu\,\omega_1 + \lambda\,\omega_2}{\lambda + \mu} .$$

Performing the integration gives

$$F_1(a) = A\,B\sqrt{\frac{2\pi}{\frac{1}{\lambda} + \frac{1}{\mu}}}\ \exp\left[-\frac{(\omega_2 - \omega_1)^2}{2(\lambda + \mu)}\right] . \qquad (4)$$

It is interesting to note that, if both the forcing function and the transfer function of the harmonic analyzer appear like bell-shaped curves, then the reading from the harmonic analyzer, as a function of the frequency deviation $(\omega_2 - \omega_1)$, is a similar bell-shaped curve, and the standard deviations of these three curves are, respectively, λ, μ, and $\lambda + \mu$.

Measurement of the Cylinder Response by a Voltmeter

If the forcing function is again represented by equation (1), and the transfer function for the cylinder response by another bell-shaped curve with "standard deviation," ν,

$$C\ \exp\left[-\frac{(\omega - \omega_3)^2}{2\nu}\right], \qquad (5)$$

then the over-all response of the cylinder to the forcing function is given by

$$A\,C\ \exp\left[-\frac{(\omega - \omega_1)^2}{2\lambda}\right]\ \exp\left[-\frac{(\omega - \omega_3)^2}{2\nu}\right] =$$

$$A\,C\ \exp\left[-\frac{(\omega_3 - \omega_1)^2}{2(\lambda + \nu)}\right]\ \exp\left[-\frac{1}{2}\left(\frac{1}{\lambda} + \frac{1}{\nu}\right)z^2\right] \qquad (6)$$

where

$$z = \omega - \frac{\nu\,\omega_1 + \lambda\,\omega_3}{\lambda + \nu} .$$

The reading of the voltmeter is the integral of this over-all value of ω, or

$$F(\omega_3 - \omega_1) = A\,C \sqrt{\frac{2\pi}{\frac{1}{\lambda} + \frac{1}{\nu}}} \exp\left[- \frac{(\omega_3 - \omega_1)^2}{2(\lambda + \nu)} \right] \tag{7}$$

Thus the reading of the voltmeter as a function of $\omega_3 - \omega_1$ is another bell-shaped curve with standard deviation $\lambda + \nu$.

Measurement of Cylinder Response by the Harmonic Analyzer

On this measurement, the harmonic analyzer is tuned to the frequency of the maximum response to the cylinder vibration for various values of the forcing frequency.

From equation (6) it is seen that the frequency for maximum response of the cylinder is that for which $z = 0$. When the harmonic analyzer is tuned to this frequency, then its transfer function becomes

$$B\ e^{-z^2/2\mu}, \tag{8}$$

and its reading becomes

$$F_2(\omega_3 - \omega_1) = A\,B\,C \exp\left[- \frac{(\omega_3 - \omega_1)^2}{2(\lambda + \nu)^2} \right] \int_{-\infty}^{\infty} \exp\left[- \frac{1}{2}\left(\frac{1}{\lambda} + \frac{1}{\nu} + \frac{1}{\mu} \right) z^2 \right] dz$$

$$= A\,B\,C \sqrt{\frac{2\pi}{\frac{1}{\lambda} + \frac{1}{\nu} + \frac{1}{\mu}}} \exp\left[- \frac{(\omega_3 - \omega_1)^2}{2(\lambda + \nu)} \right] .$$

Thus, for this case, the reading of the harmonic analyzer as a function of $\omega_3 - \omega_1$ is again a bell-shaped curve with the same "mean deviation," $\lambda + \nu$, as was obtained with the voltmeter.

Conclusions

Experiments indicated that all three measurements have roughly the same band width, i.e., $\lambda + \mu = \lambda + \nu$. The implication is that $\nu = \mu$.

To estimate μ, we note from the Instruction Manual of the Hewlett-Packard Model 300 A Harmonic Wave Analyzer that the band width for an attenuation of the voltage to $1/\sqrt{2}$ of the resonance peak (which approximates μ) is about 6.5 cycles. The average measured band width of the frequency response curves at an amplitude ratio of $1/\sqrt{2}$ appears to be about 5-6 cycles according to the data presented in Figures 13-15. These results indicate that the forcing function (oscillator) has a much narrower band width than either the analyzer or the cylinder. Hence we may conclude that the transfer function of the cylinder, being a bell-shaped curve, has a band width of approximately 6 cycles at $1/\sqrt{2}$ amplitude ratio, regardless of the frequency range. Since the damping coefficient, g, ordinarily used in aircraft engineering, is equal to the band width at $1/\sqrt{2}$ amplitude ratio divided by the natural frequency, the experimental result shows that the g-values so determined will vary with frequency. In other words, the damping characteristics of the test specimens cannot be expressed as a constant structural damping coefficient. The result can be expressed by saying that

$$gf = 6 \text{ cycles},$$

where f is the frequency in cycles per second.

REFERENCES

1. Arnold, R. N. and Warburton, G. B., "Flexural Vibrations of the Walls of Thin Cylindrical Shells Having Freely Supported Ends," Proceedings of the Royal Society (London), Series A, Vol. 197, 1949, p. 238.

2. Arnold, R. N. and Warburton, G. B., "The Flexural Vibrations of Thin Cylinders," Journal and Proceedings of the Institution of Mechanical Engineers (London), Vol. 167, 1953, pp. 62-74.

3. Reissner, E., Non-Linear Effects in Vibrations of Cylindrical Shells, Ramo-Wooldridge GMRD Aeromechanics Section Report AM 5-6, August 1955.

4. Fung, Y. C., On the Vibration of Thin Cylindrical Shells Under Internal Pressure, Ramo-Wooldridge GMRD Aeromechanics Section Report AM 5-8, September 1955.

5. Tobias, S. A., "A Theory of Imperfection for the Vibration of Elastic Bodies of Revolution," Engineering, Vol. 172, 1951, p. 409.

2

FRAMES

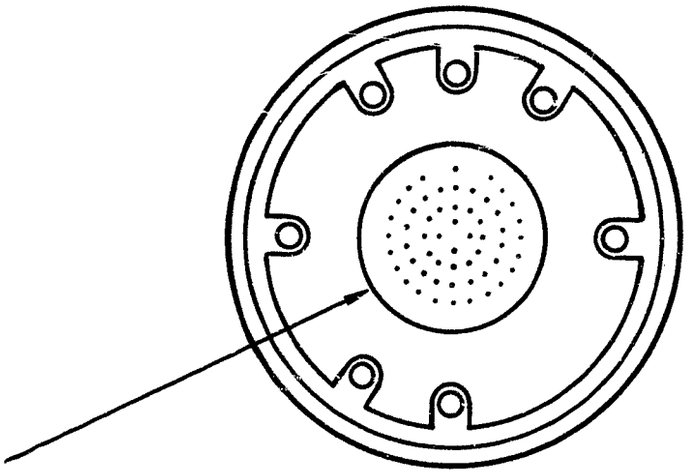

6 WIRE CONNECTOR

SECTION DD

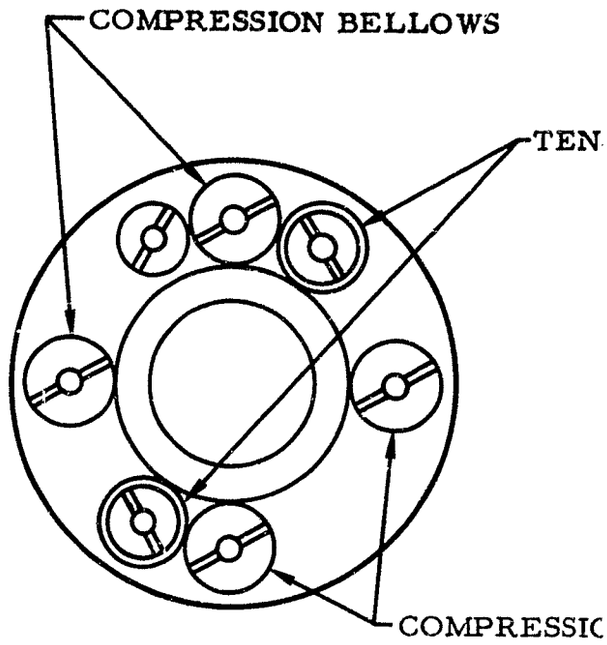

SECTION CC

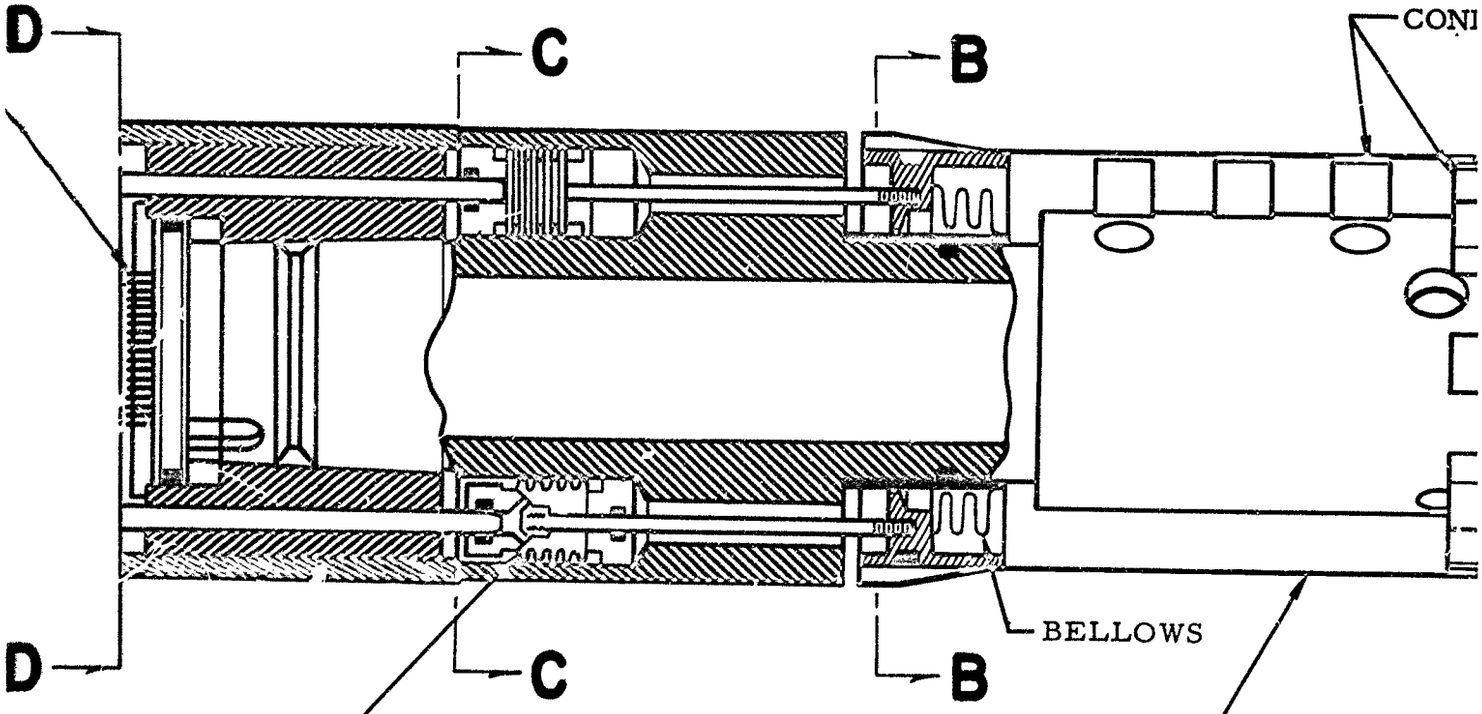

NOTE: SECTION IS ROTATED TO SHOW SKIN TENSIONING BELLOWS ASSEMBLY

11" SKIN .001
.002
.003

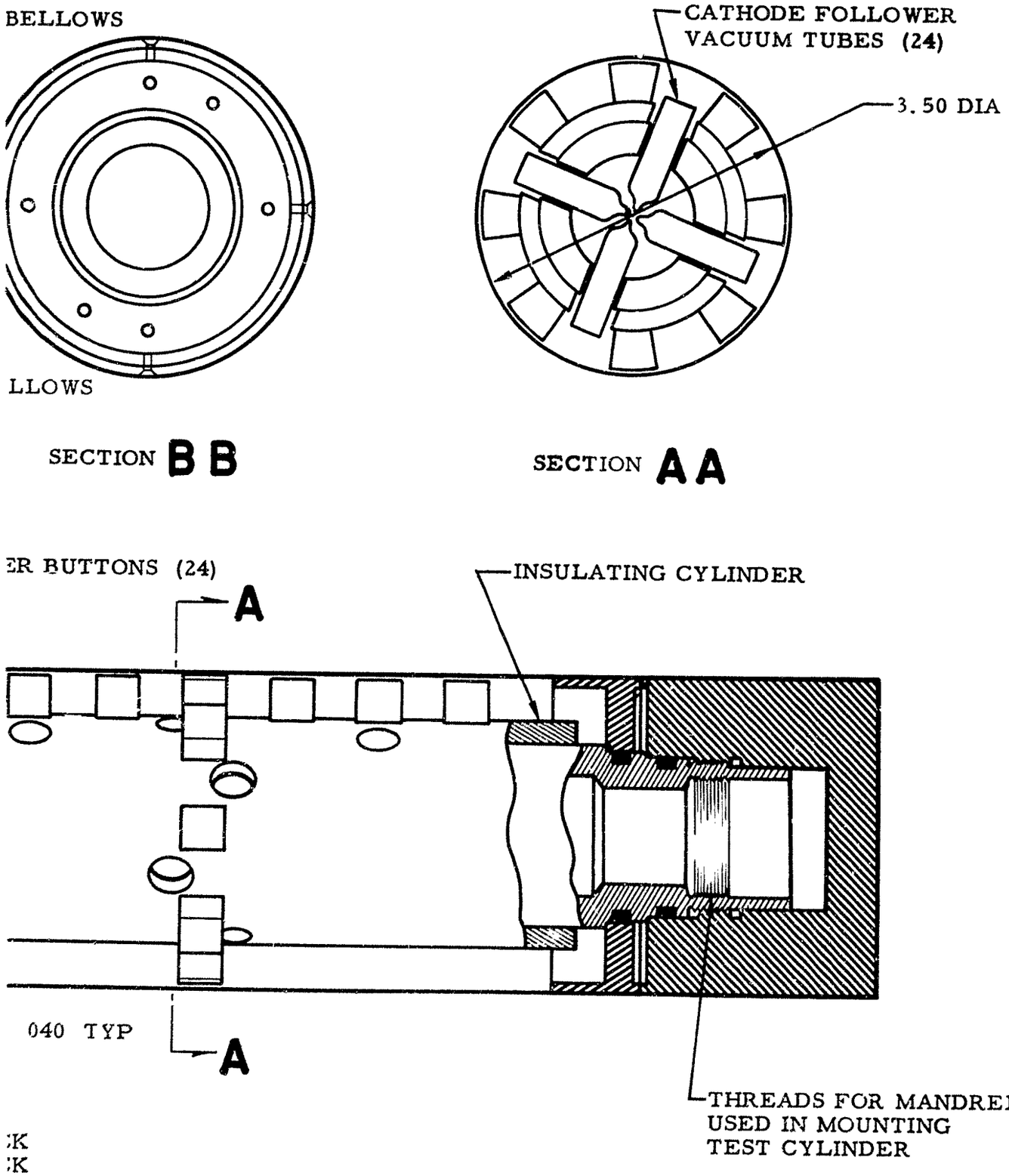

FIG. 1 TEST SPECIMEN, PRESSURIZATION SYSTEM, AND

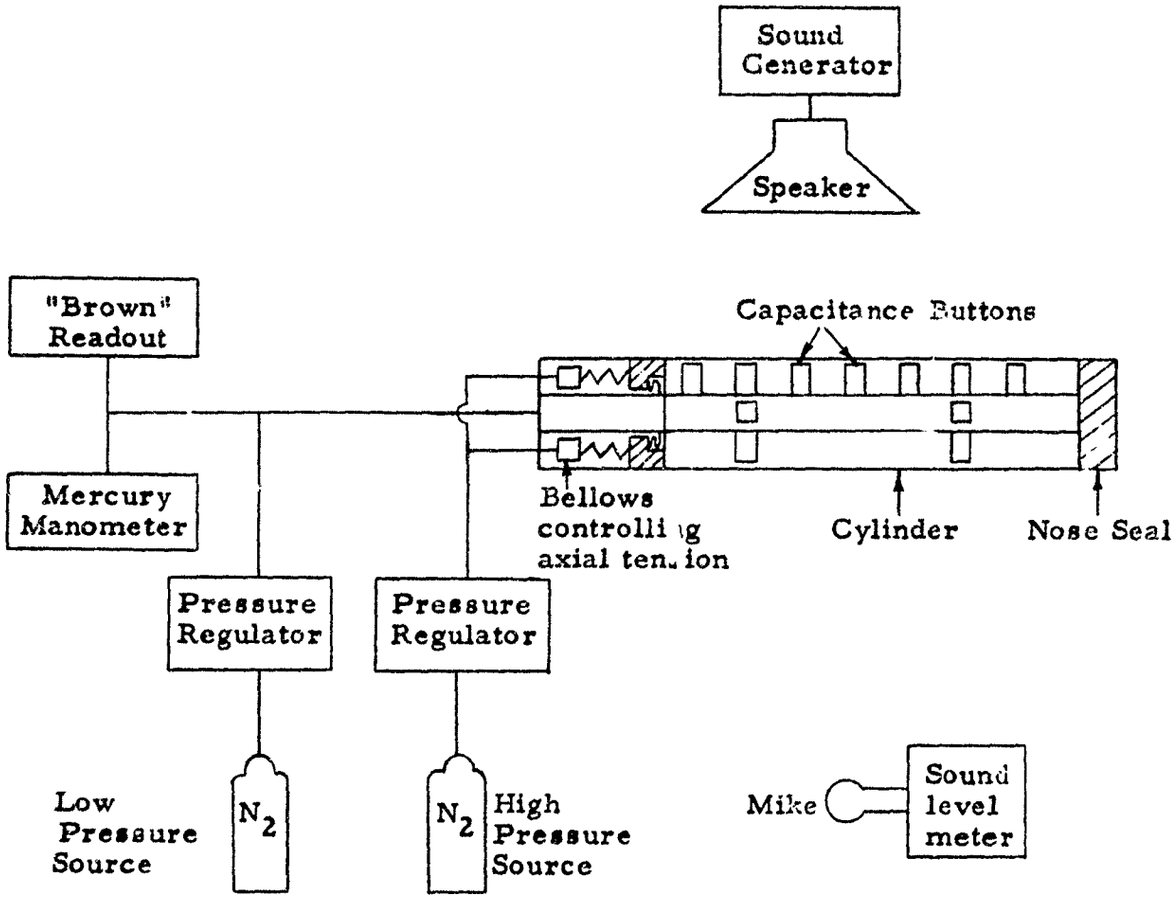

Fig. 2

Schematic Diagram of Test Set-up

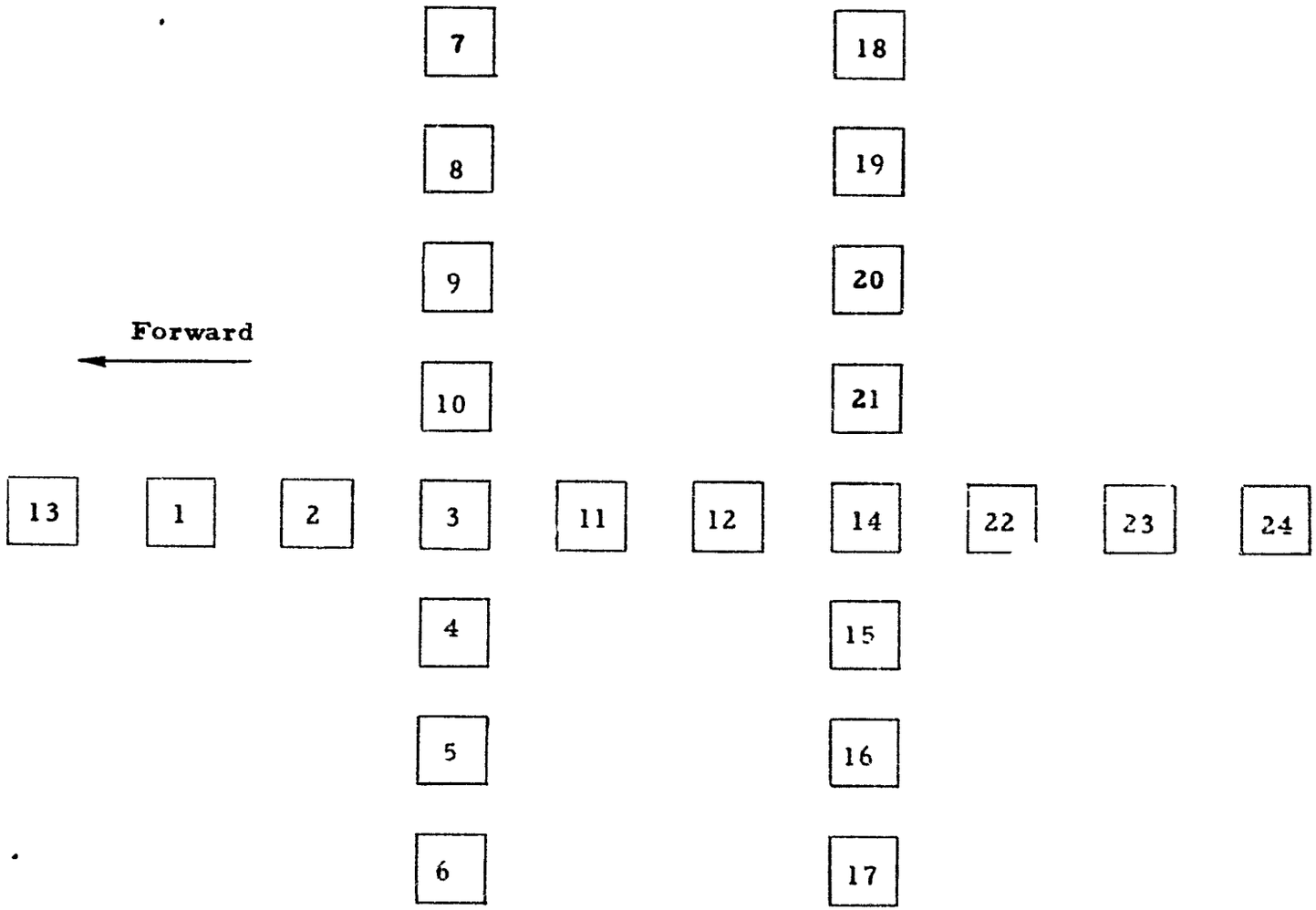

Figure 3
Identification of Pick-up Buttons
Top View of Developed Surface

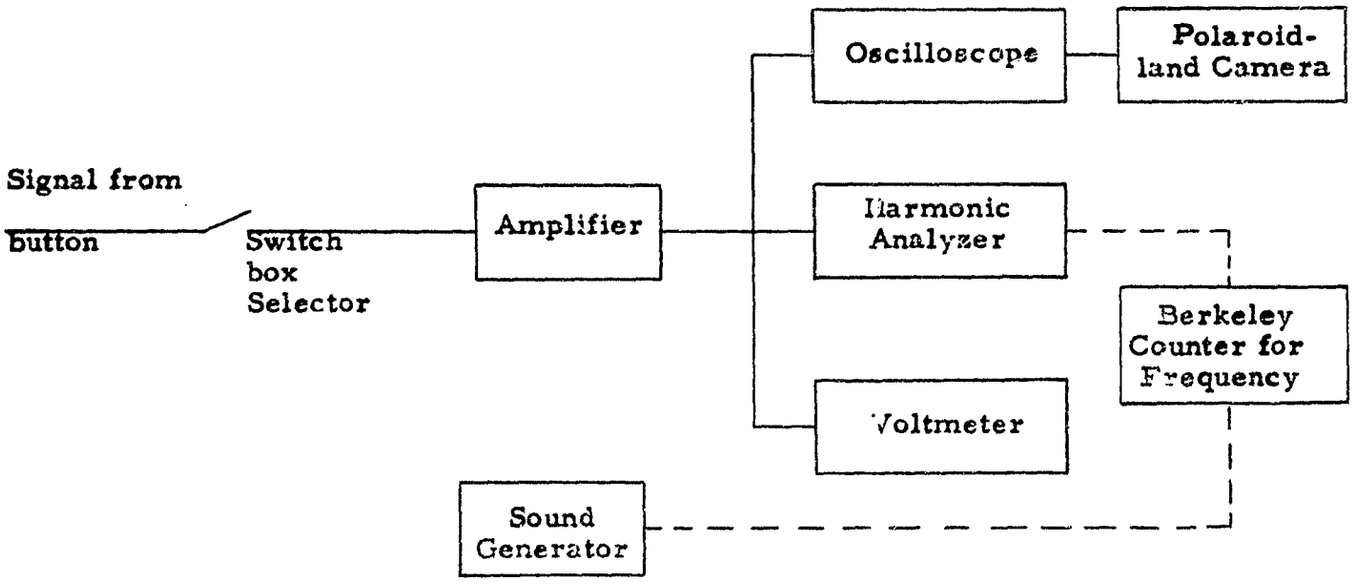

Fig. 4

Schematic Diagram of Instrumentation

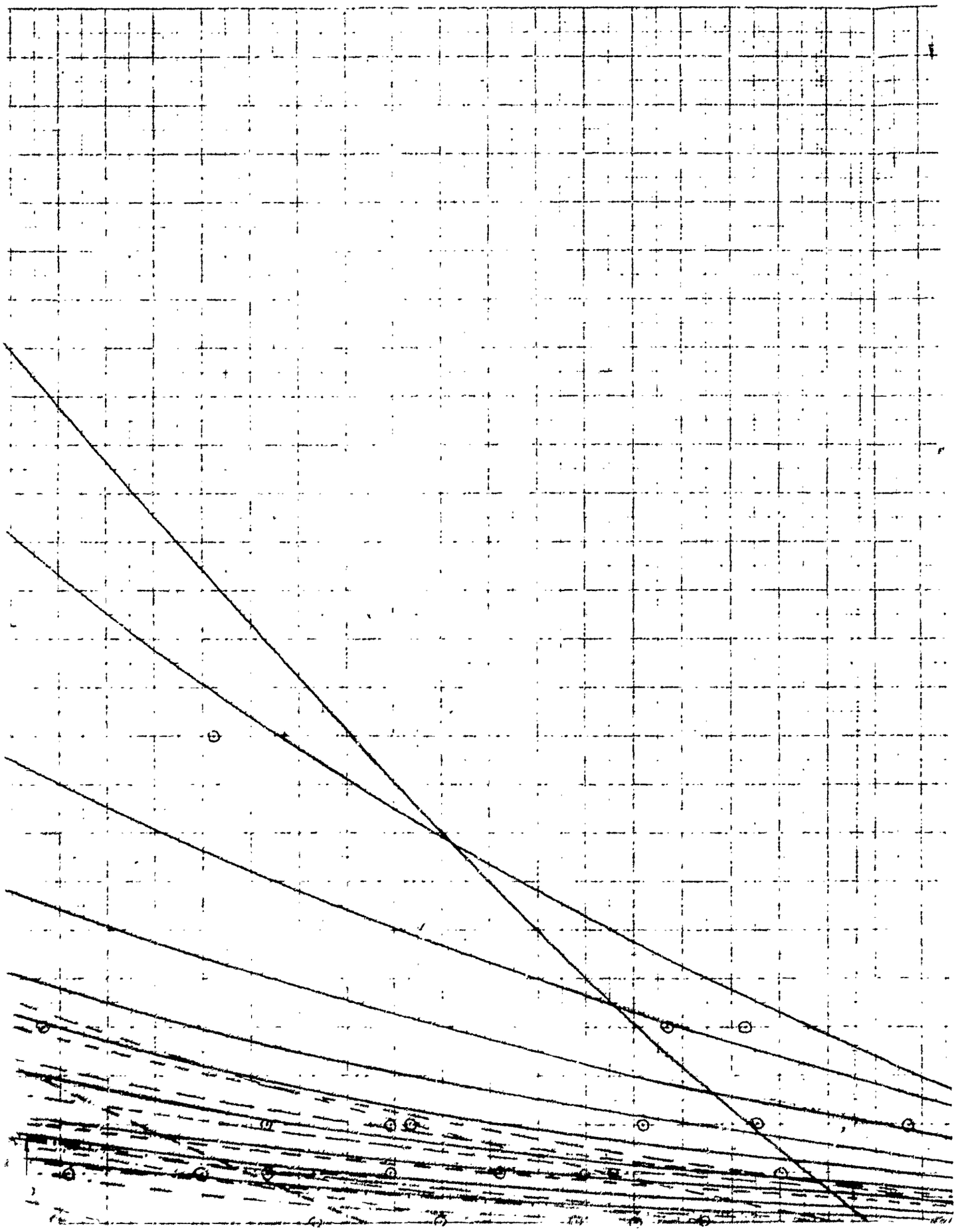

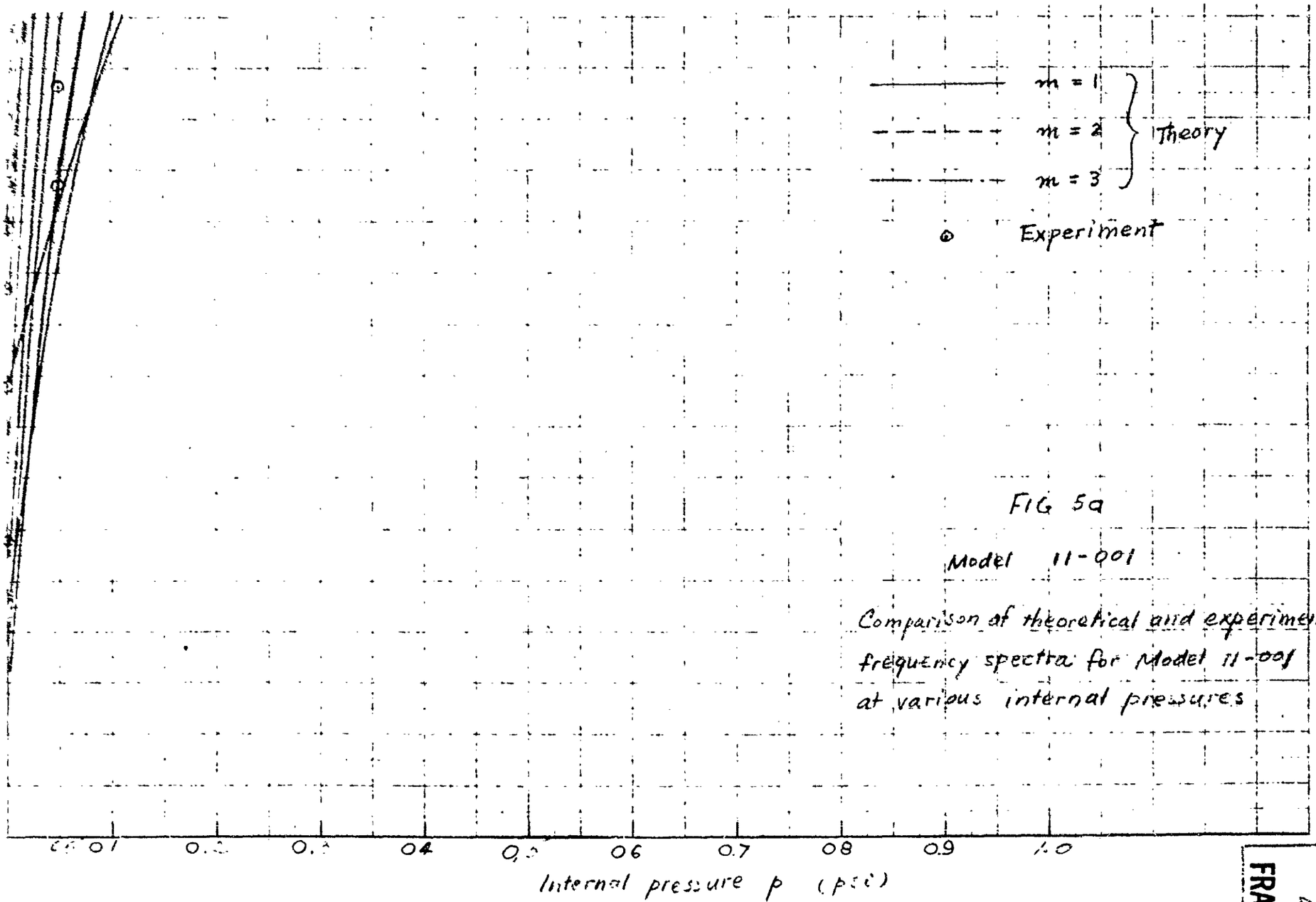

FIG 5a

Model 11-001

Comparison of theoretical and experimental frequency spectra for Model 11-001 at various internal pressures

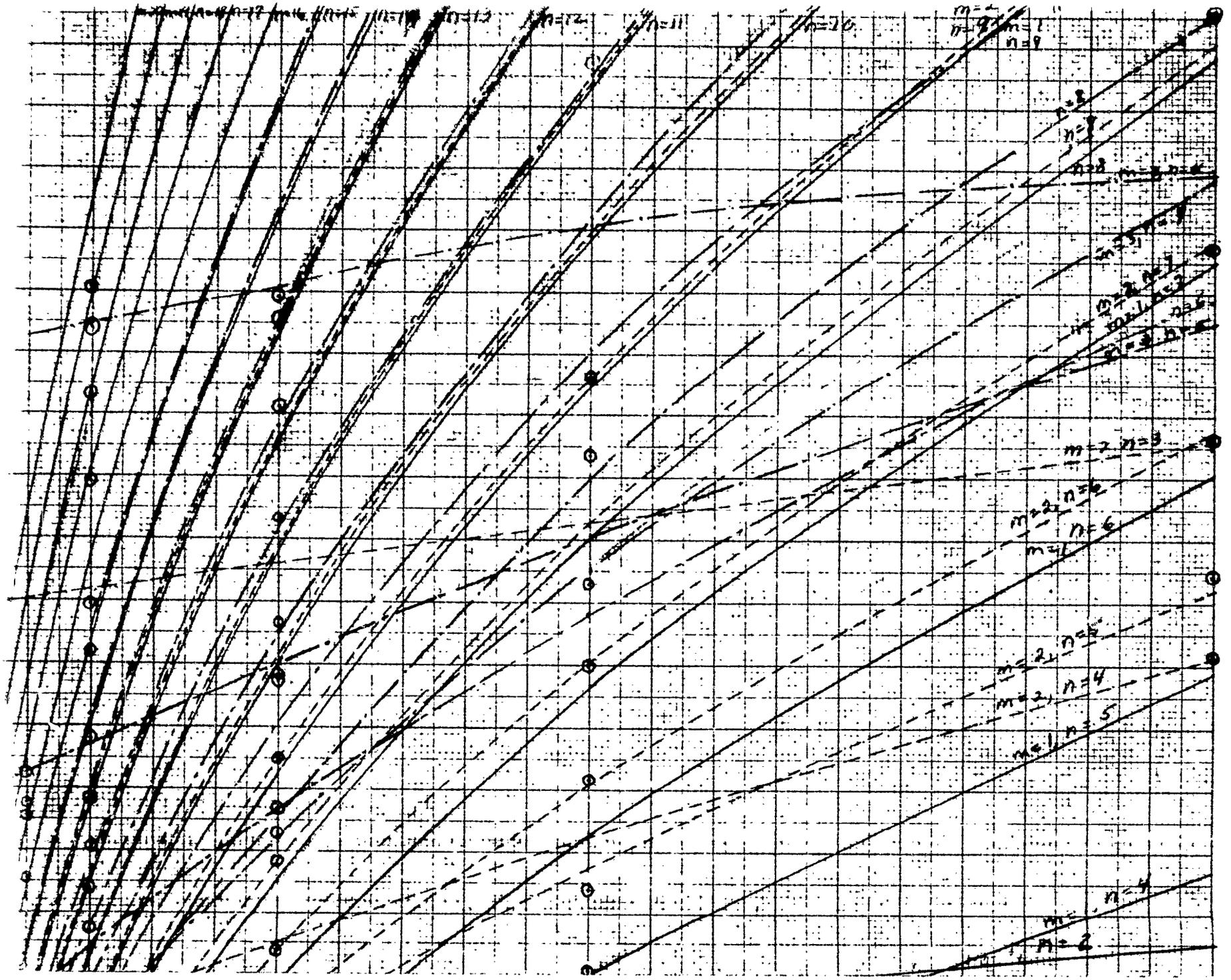
m=1 n=9
m=2 n=8
m=3 n=7
m=4 n=6
m=5 n=5
m=6 n=4
m=7 n=3
m=8 n=2
m=9 n=1

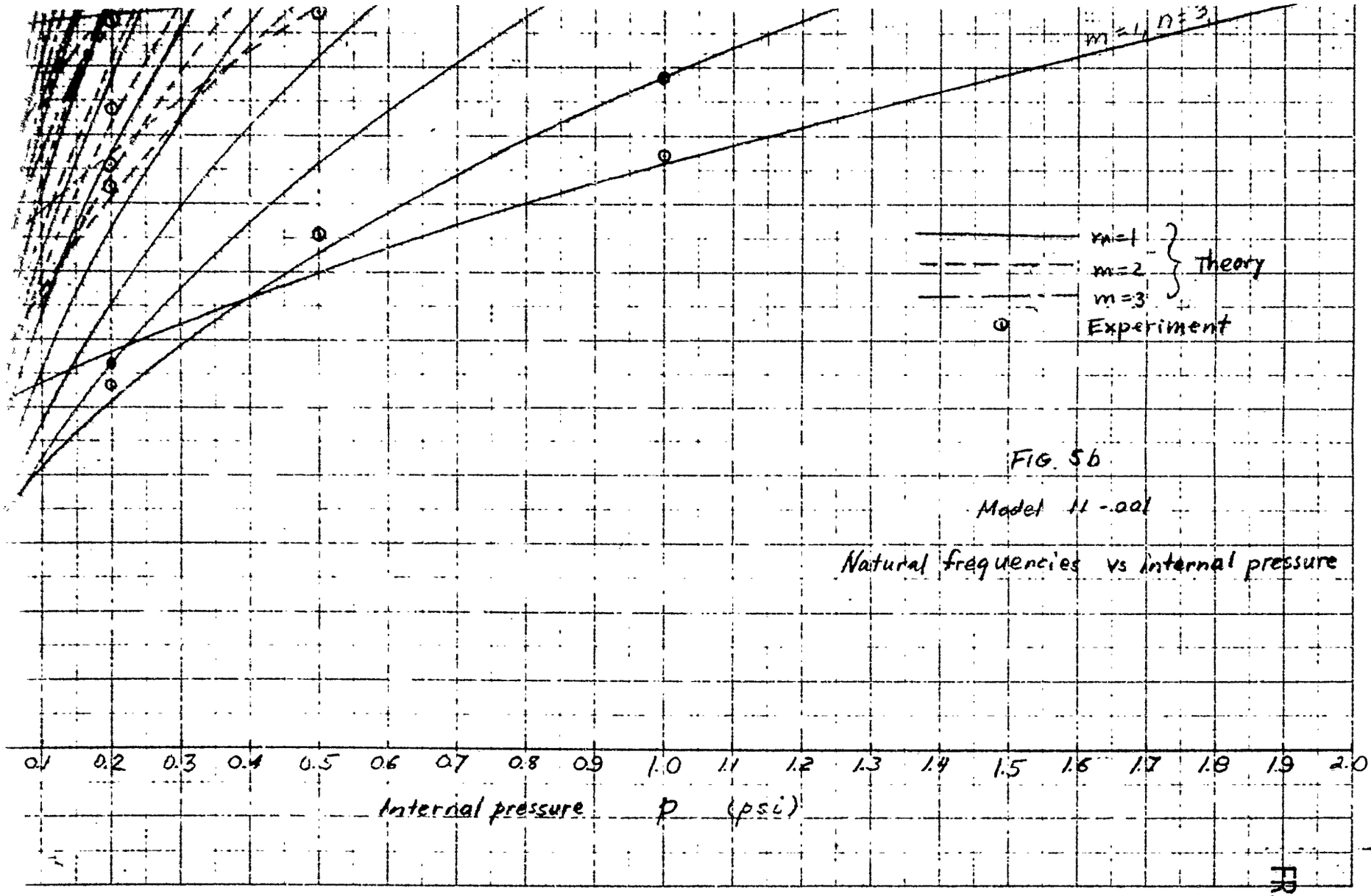

FIG. 5b

Model 11-aal

Natural frequencies vs internal pressure

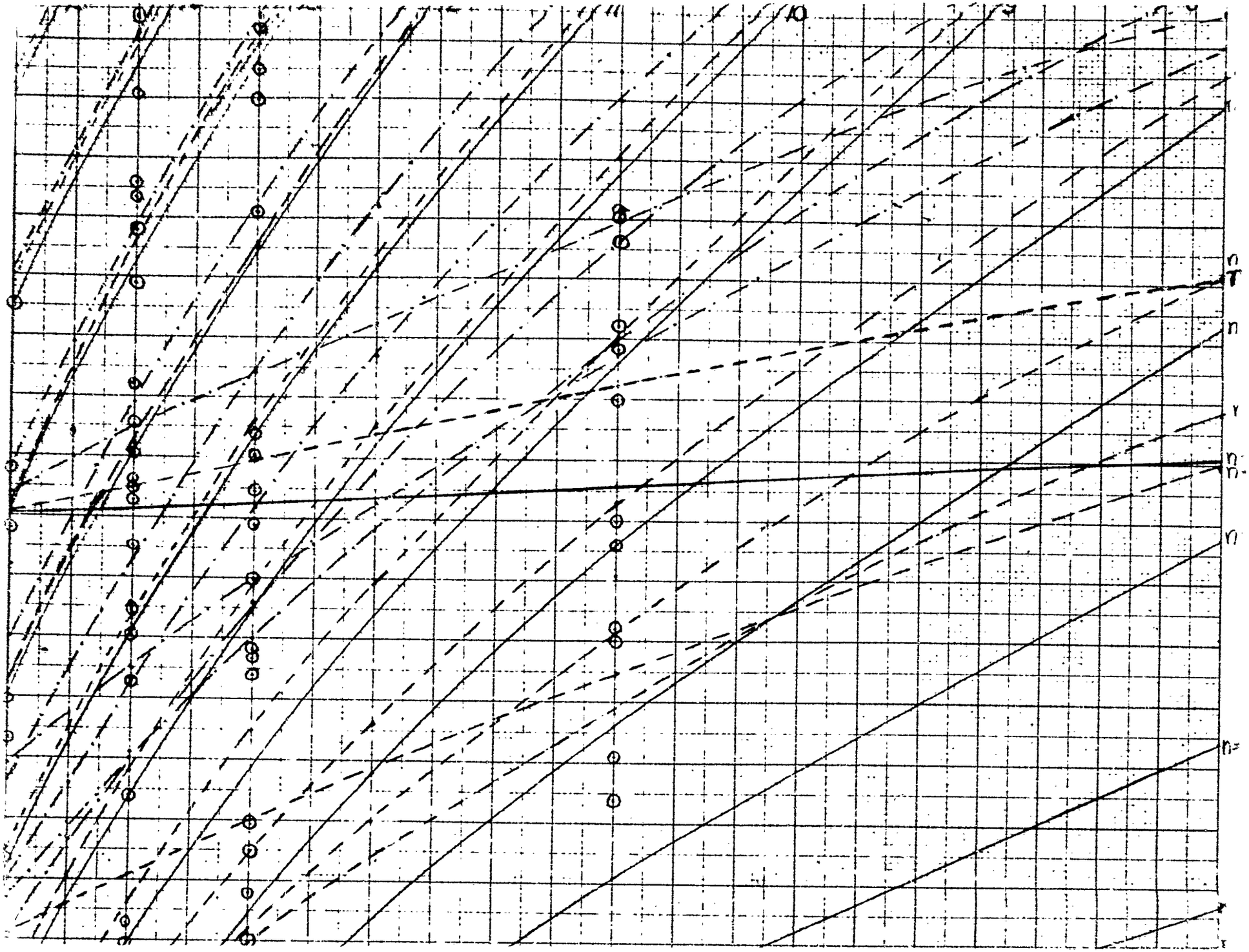

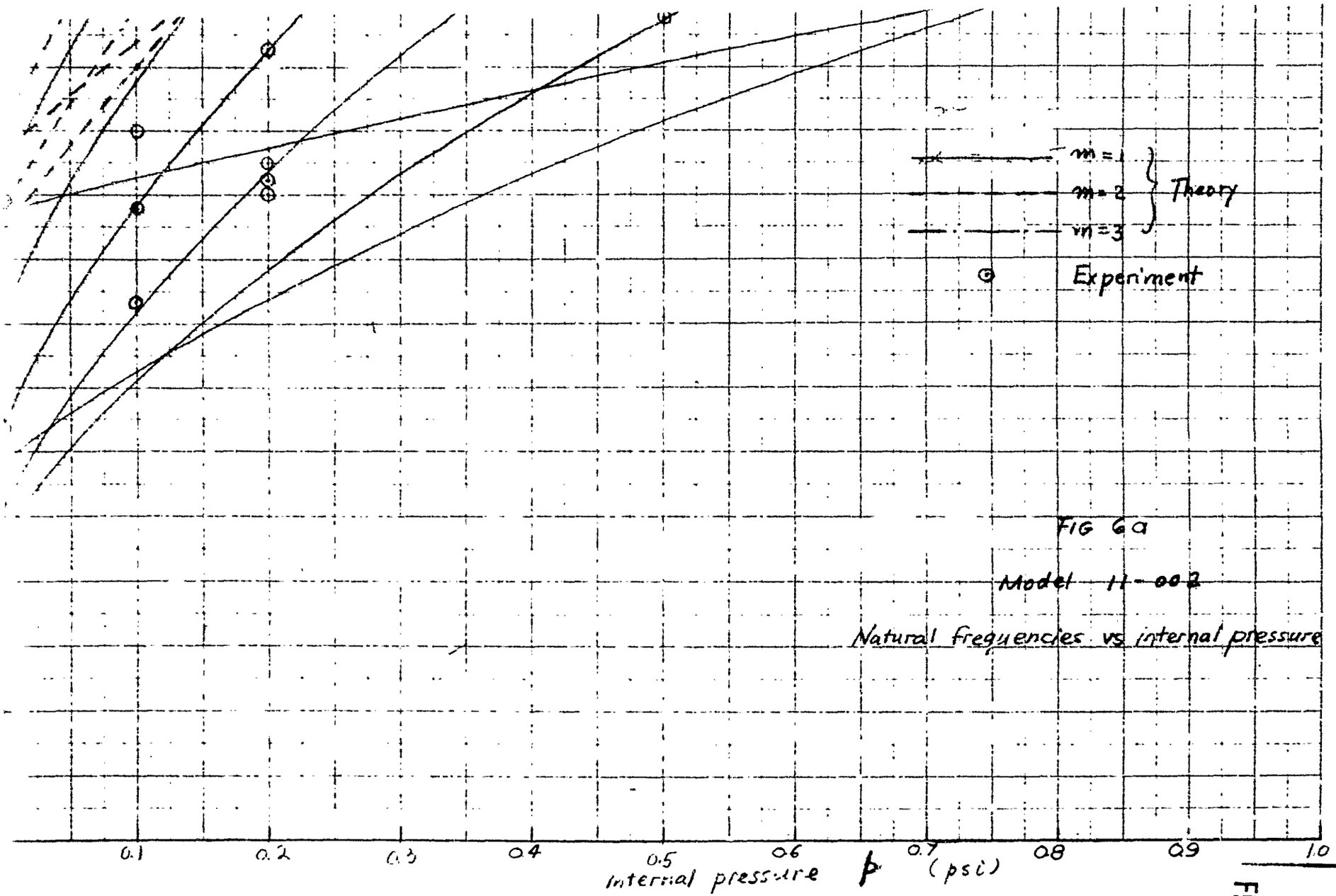

FIG 6a

Model 11-002

Natural frequencies vs internal pressure

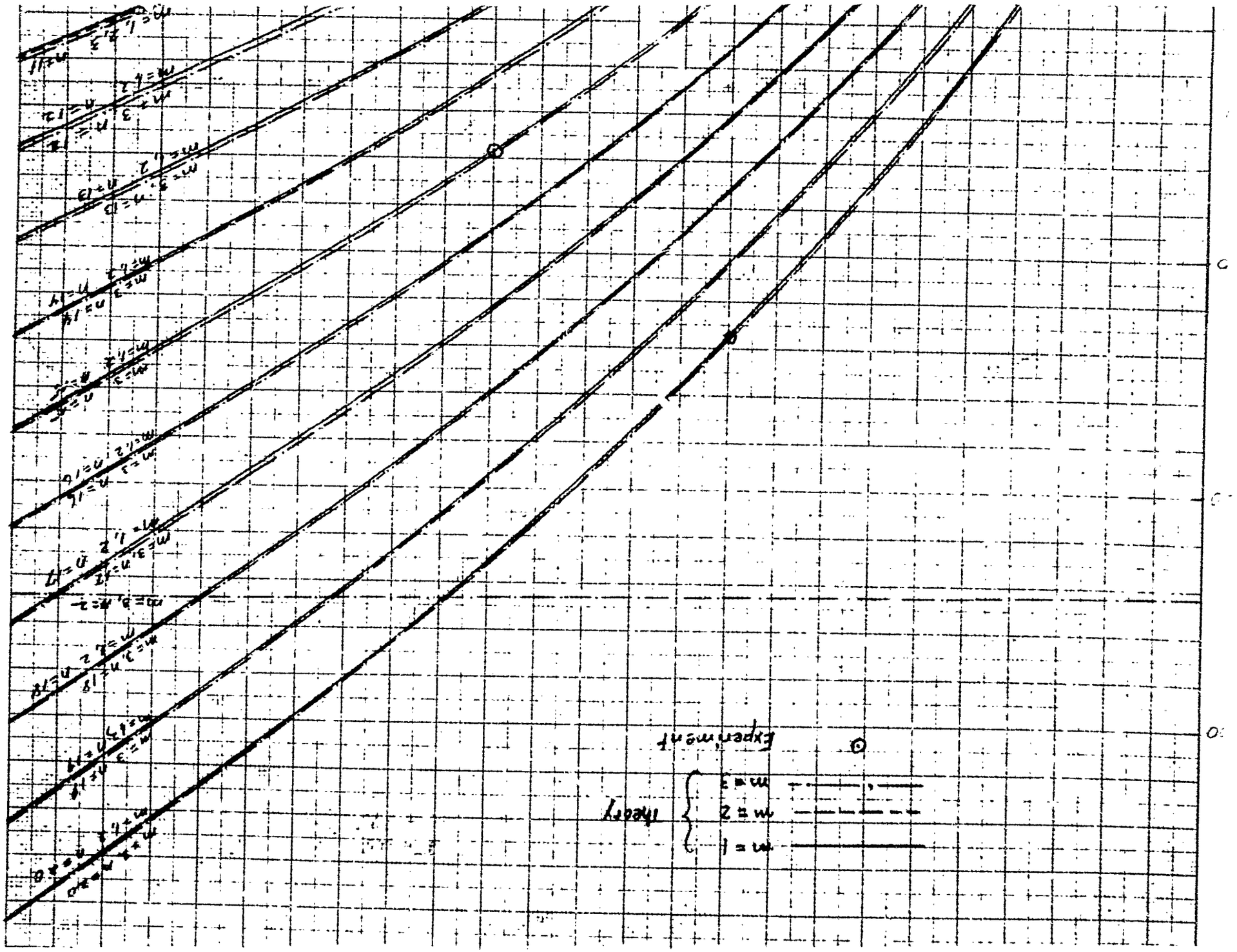
Experiment
Theory
m = 3
m = 2
m = 1

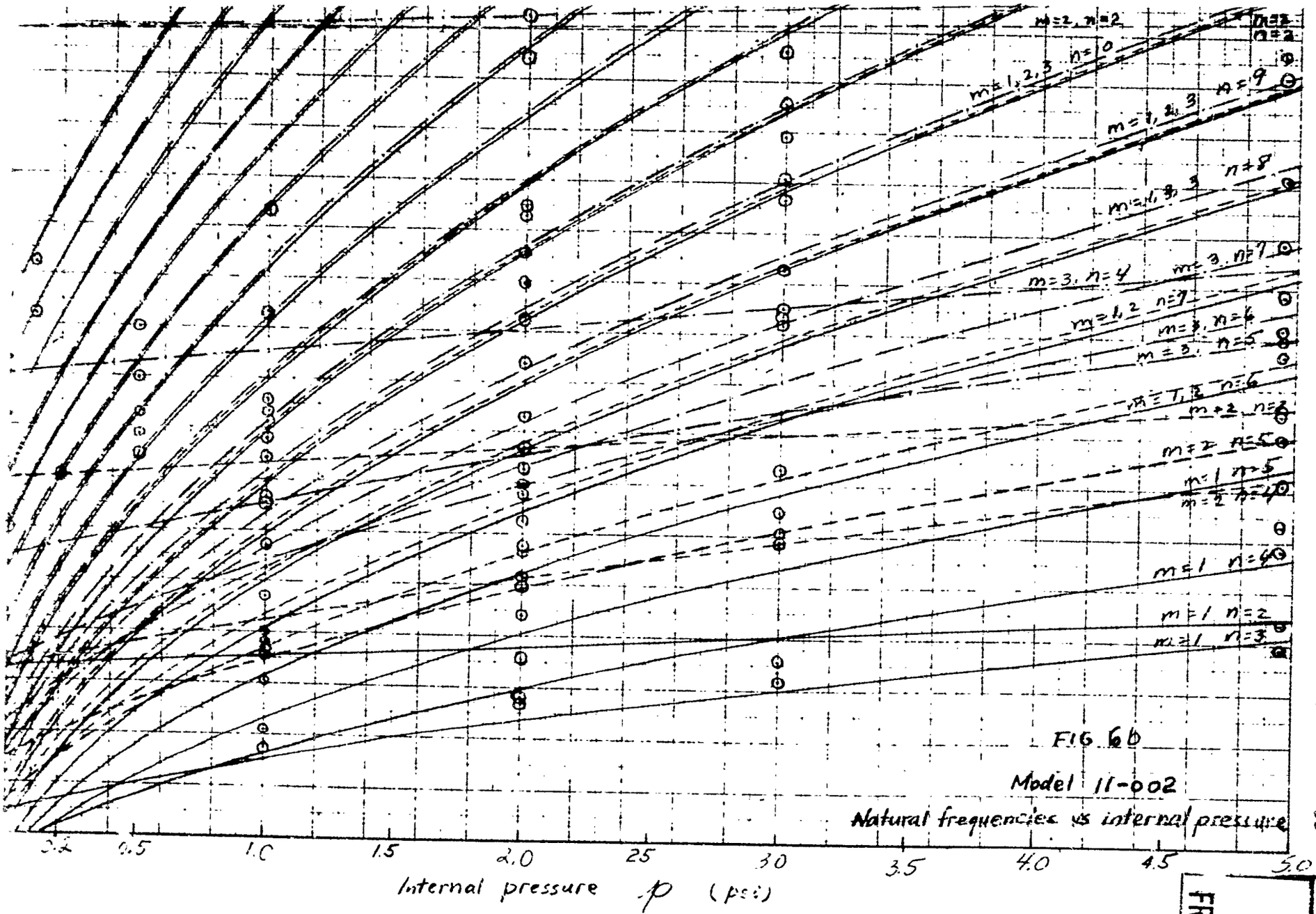

FIG. 6b

Model 11-002

Natural frequencies vs internal pressure

FRAMES 2

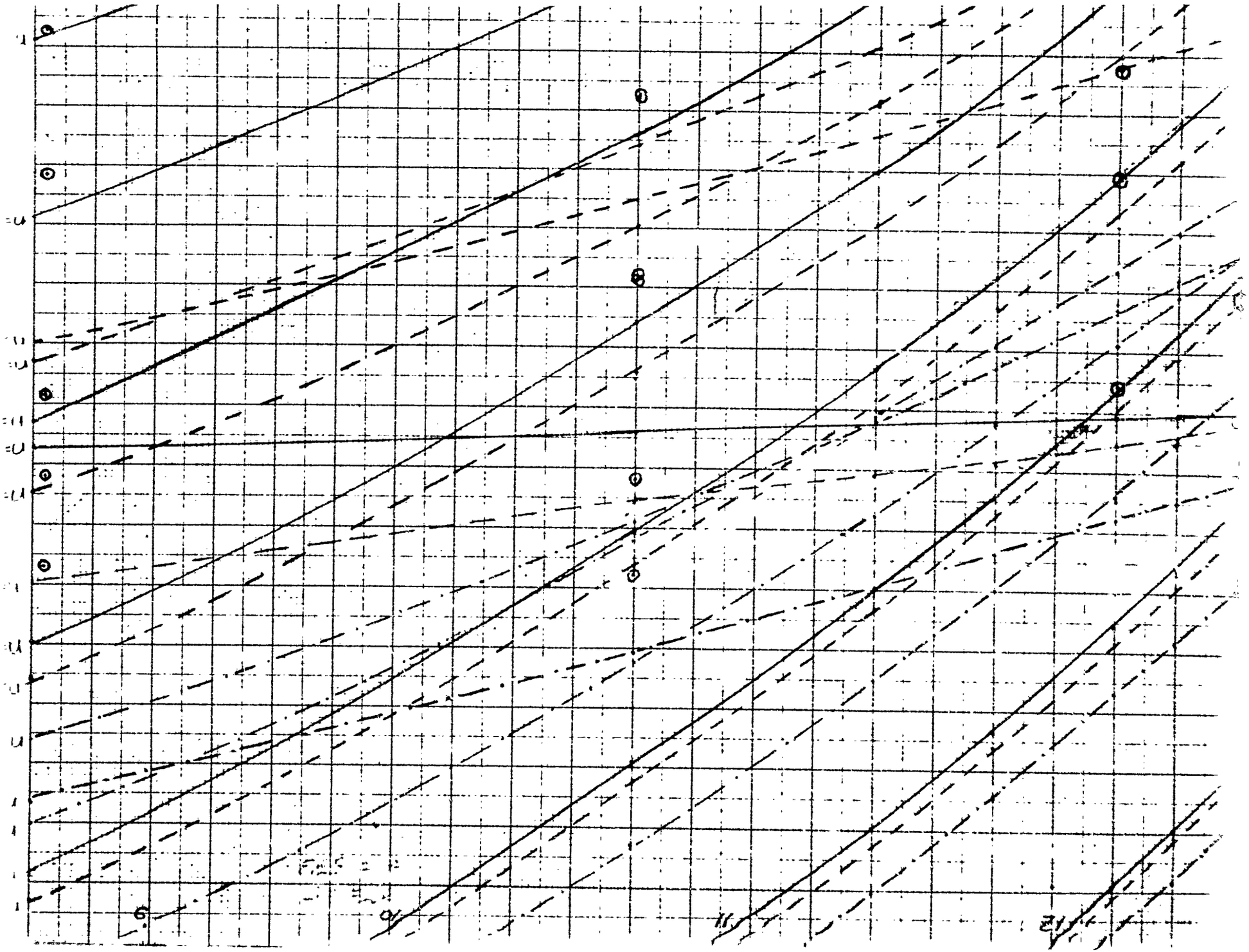

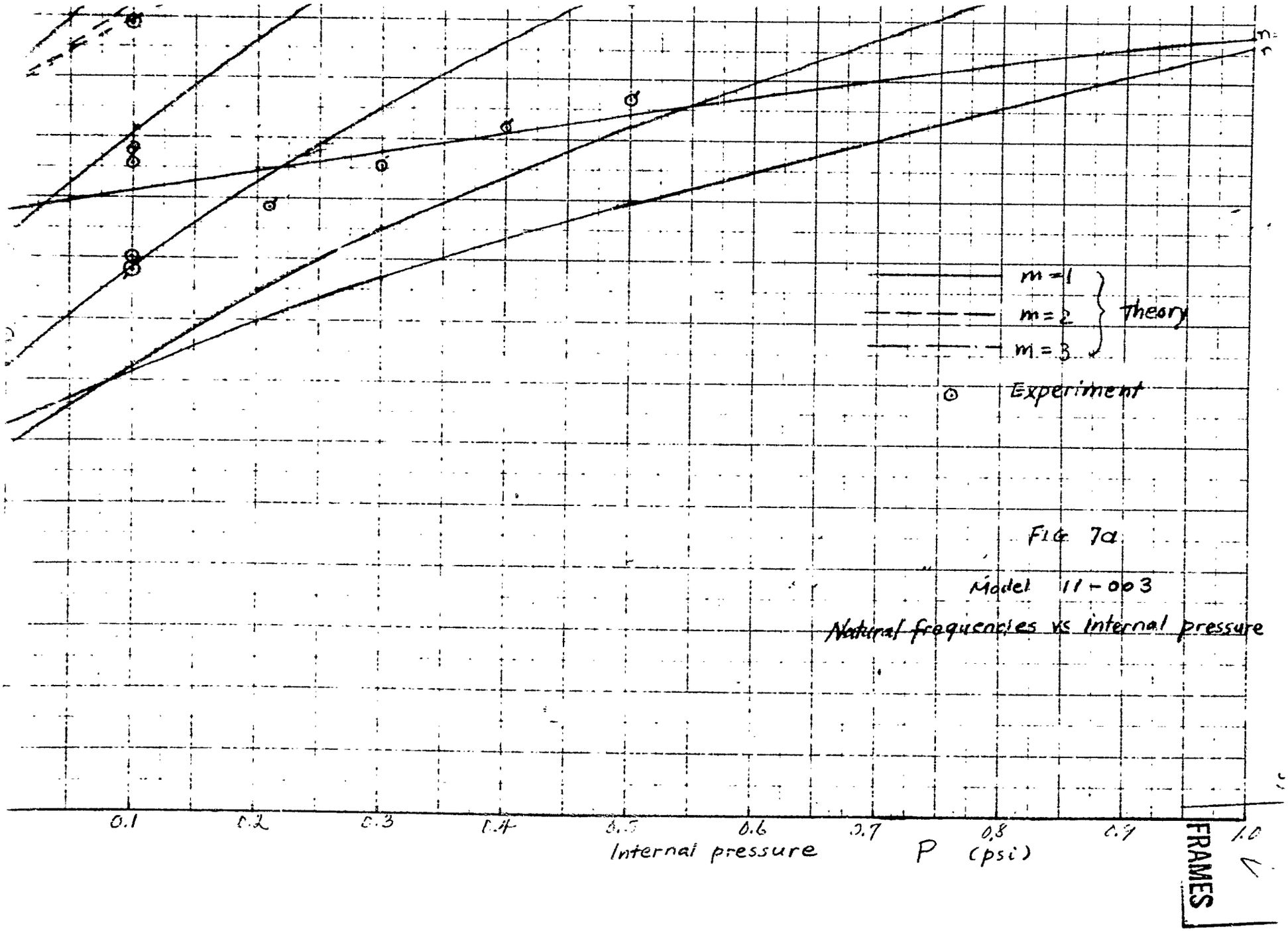

Fig 7a

Model 11-003

Natural frequencies vs internal pressure

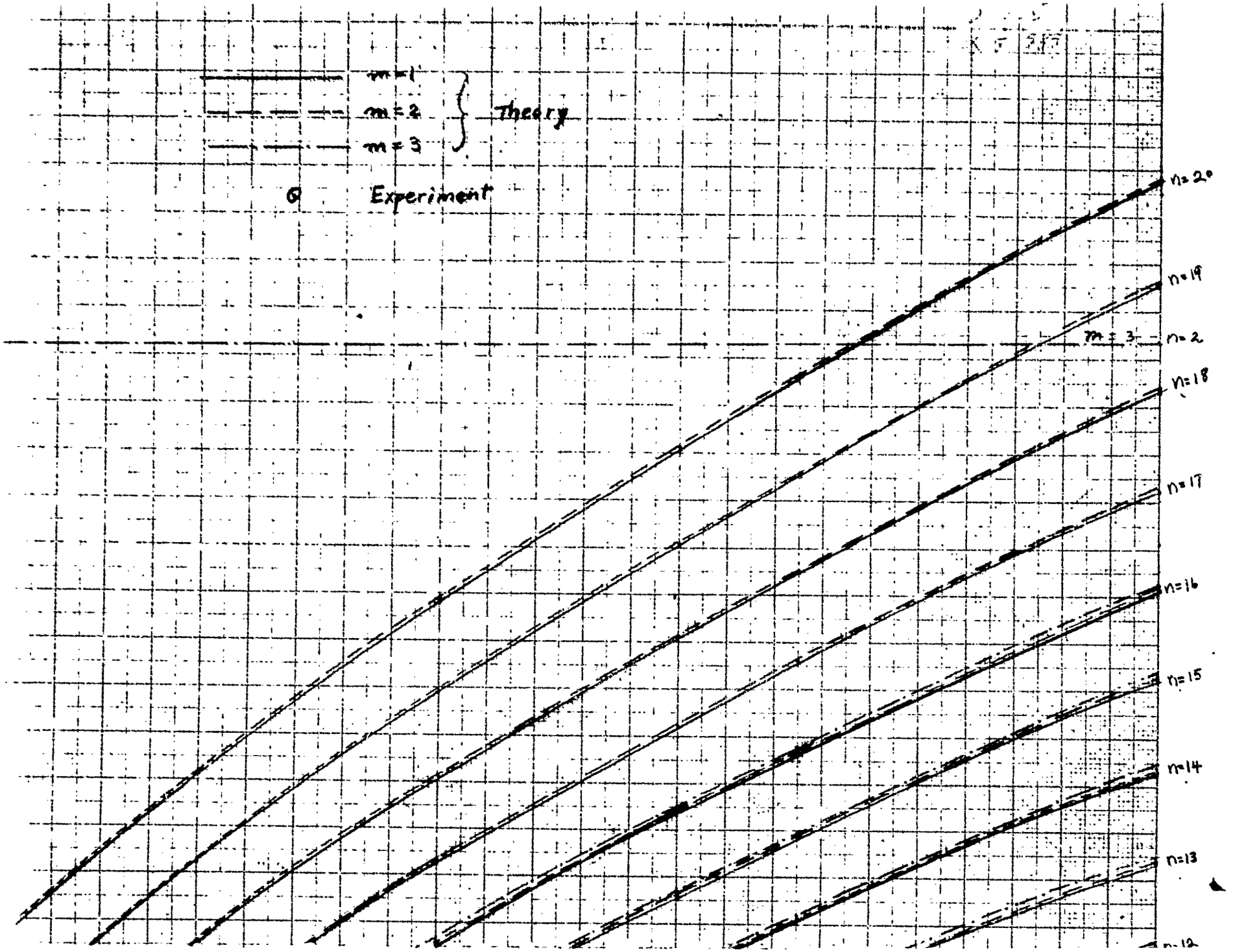
m = 1
m = 2
m = 3
Theory
Experiment
n = 20
n = 19
m = 3
n = 2
n = 18
n = 17
n = 16
n = 15
n = 14
n = 13

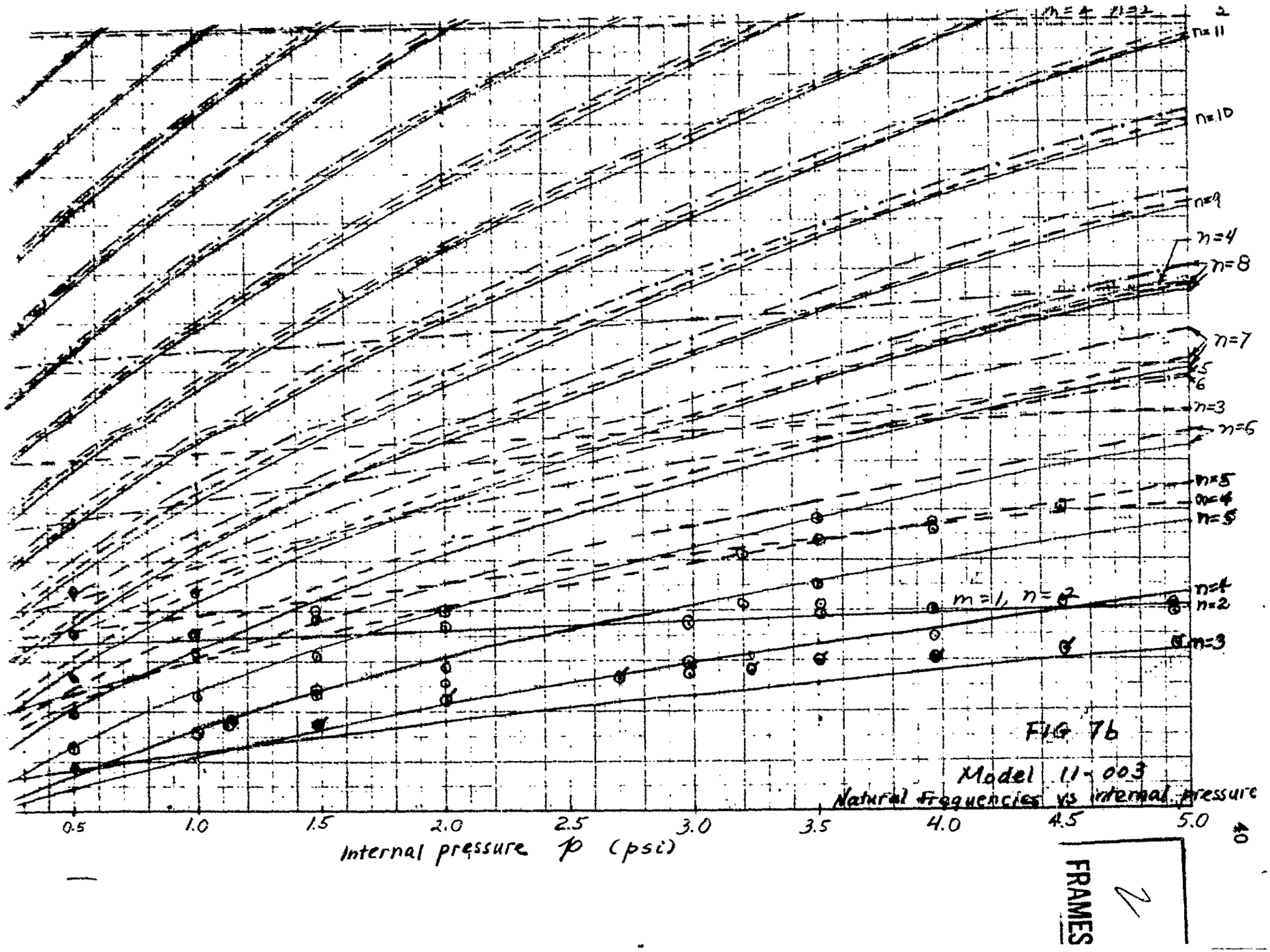

FIG 7b

Model 11-003

Natural frequencies vs internal pressure

FRAMES 2

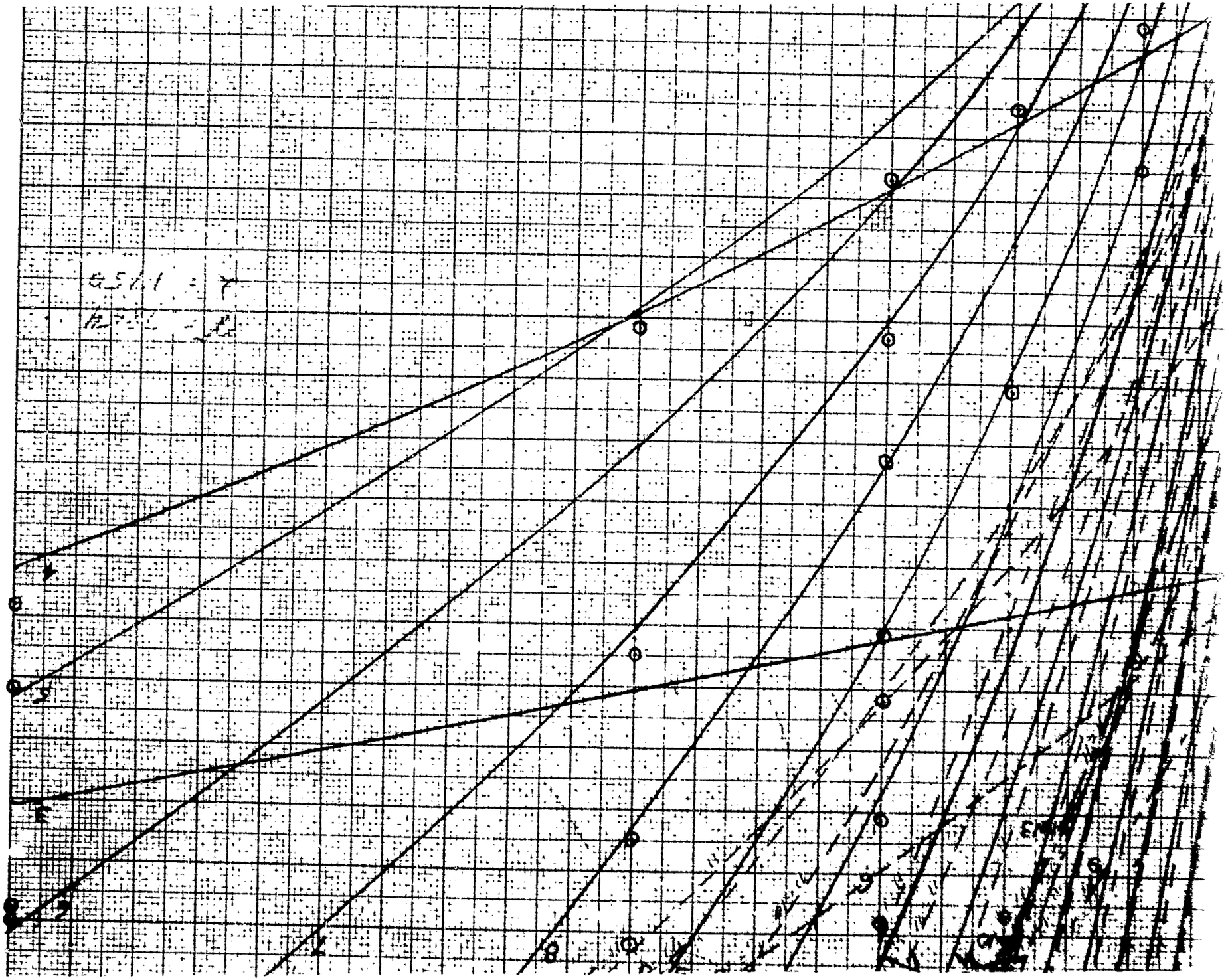

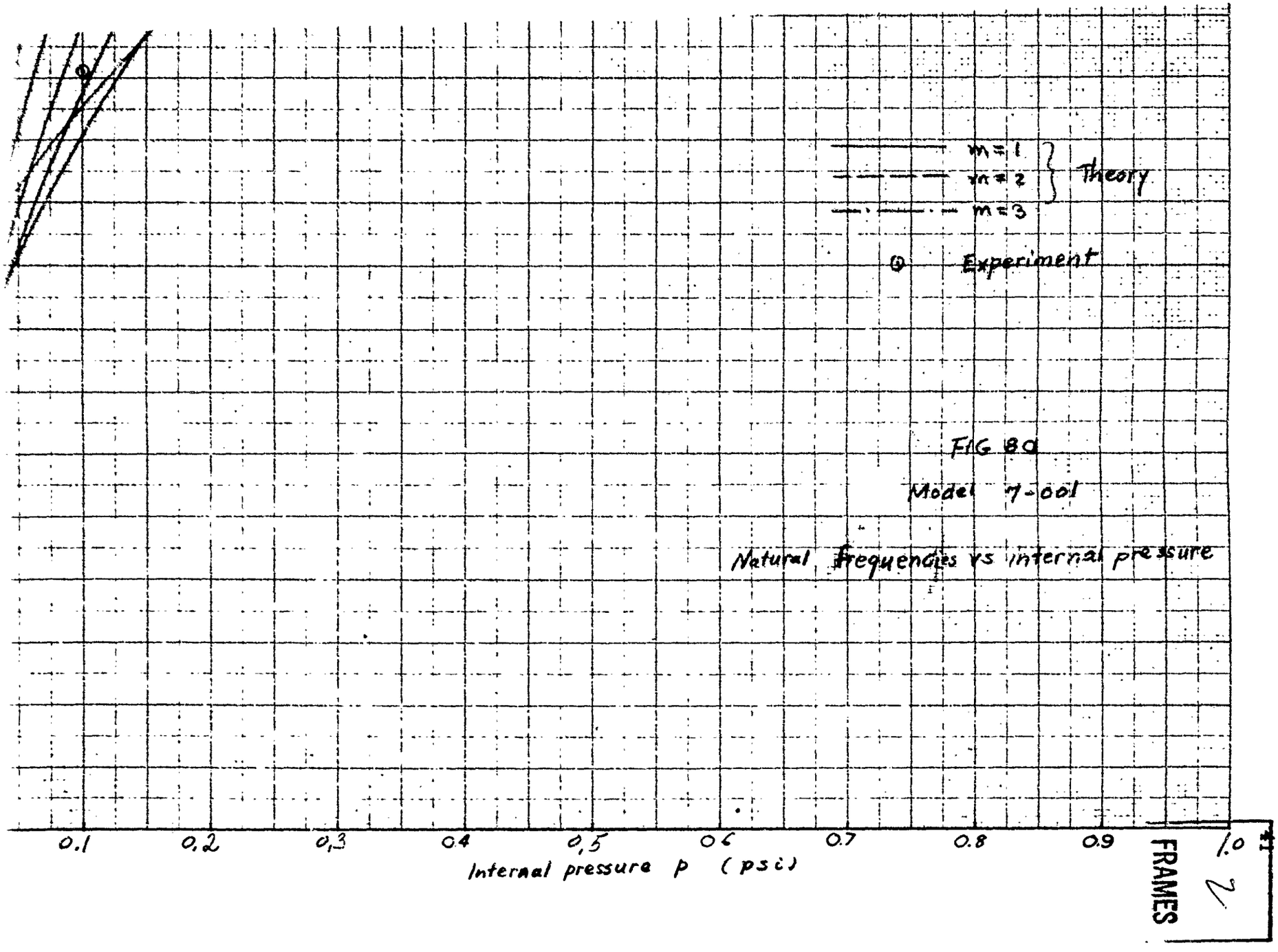

FIG 8a

Model 7-001

Natural frequencies vs internal pressure

FRAMES

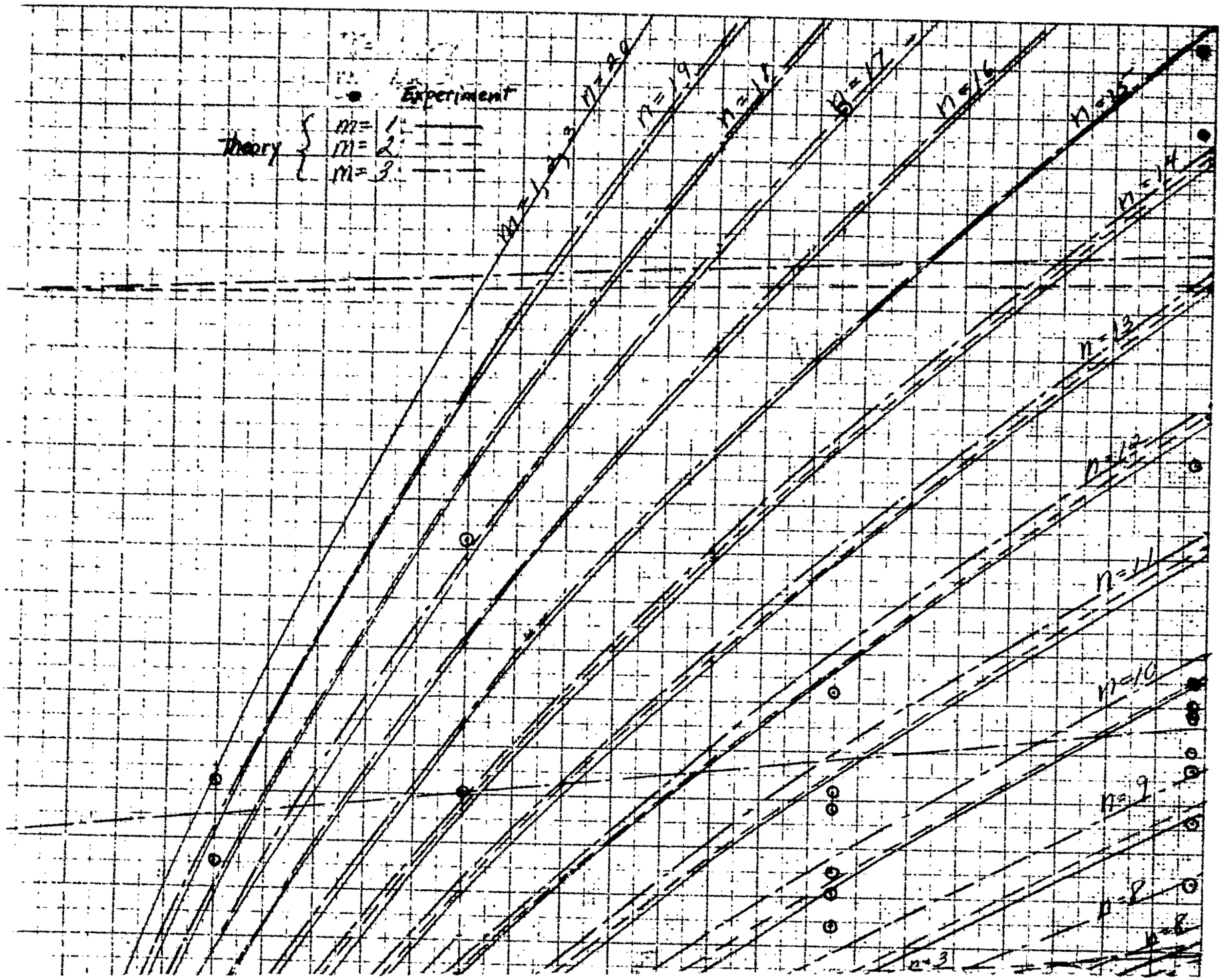
Experiment
Theory
m= 1
m= 2
m= 3
n=20
n=19
n=18
n=17
n=16
n=15
n=14
n=13
n=12
n=11
n=10
n=9
n=8
n=7
n=6
n=5
n=4
n=3

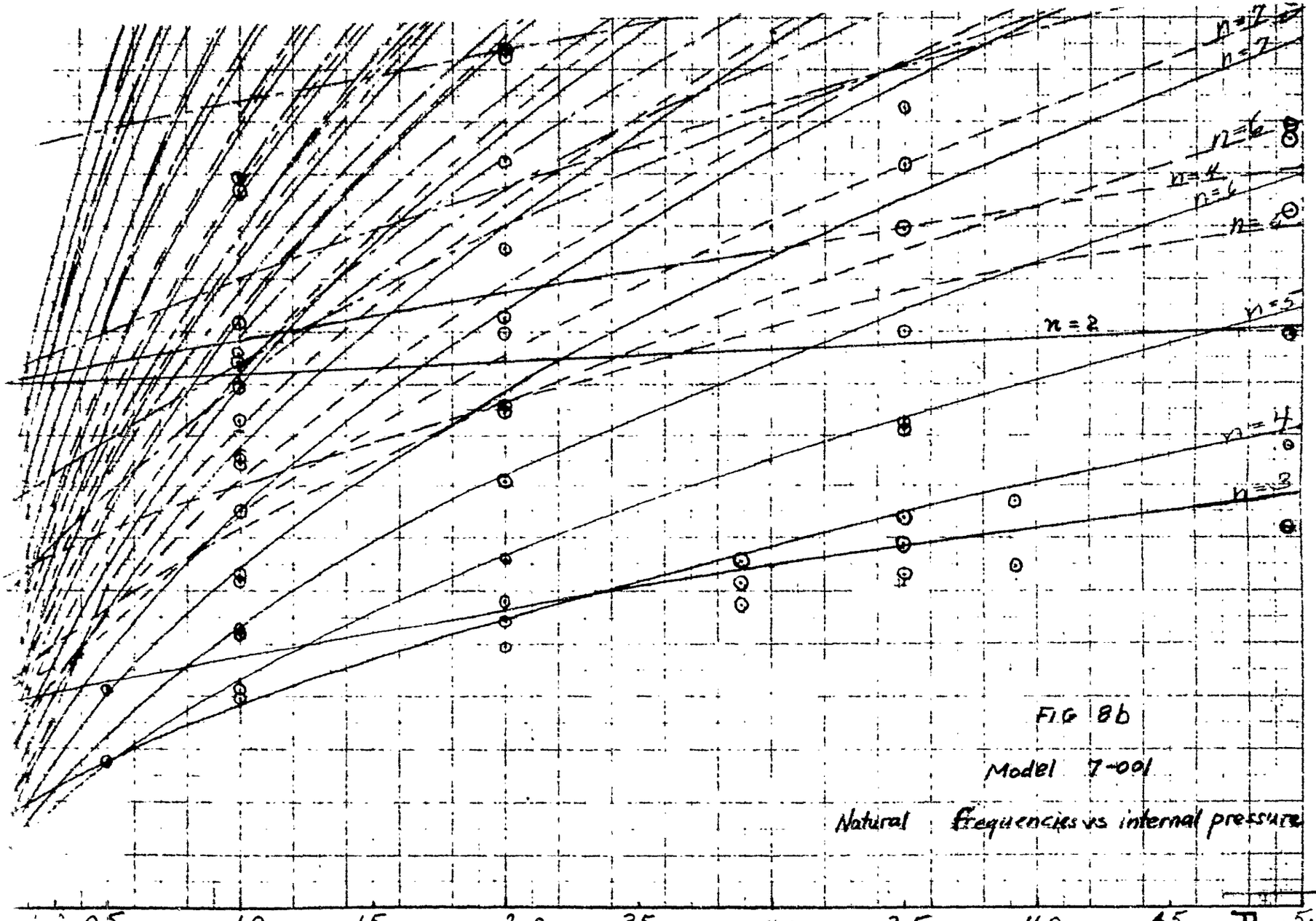

FIG 8b

Model 7-001

Natural frequencies vs internal pressure

FRAMES 42

15
16
17
18
19
20

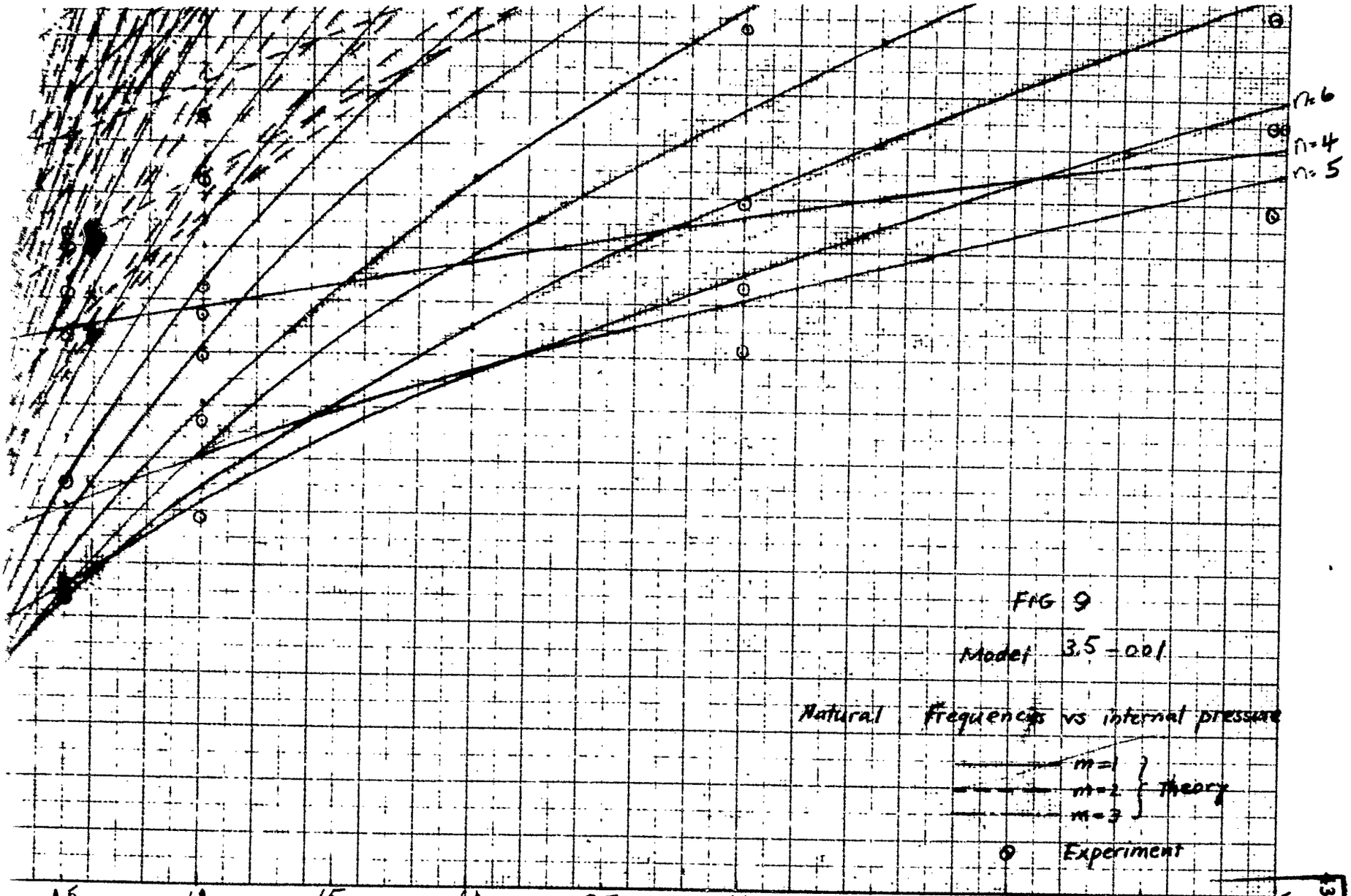

FIG 9

Model 3.5 - 001

Natural Frequencies vs internal pressure

m=1 } theory
m=2 }
m=3 }

Experiment

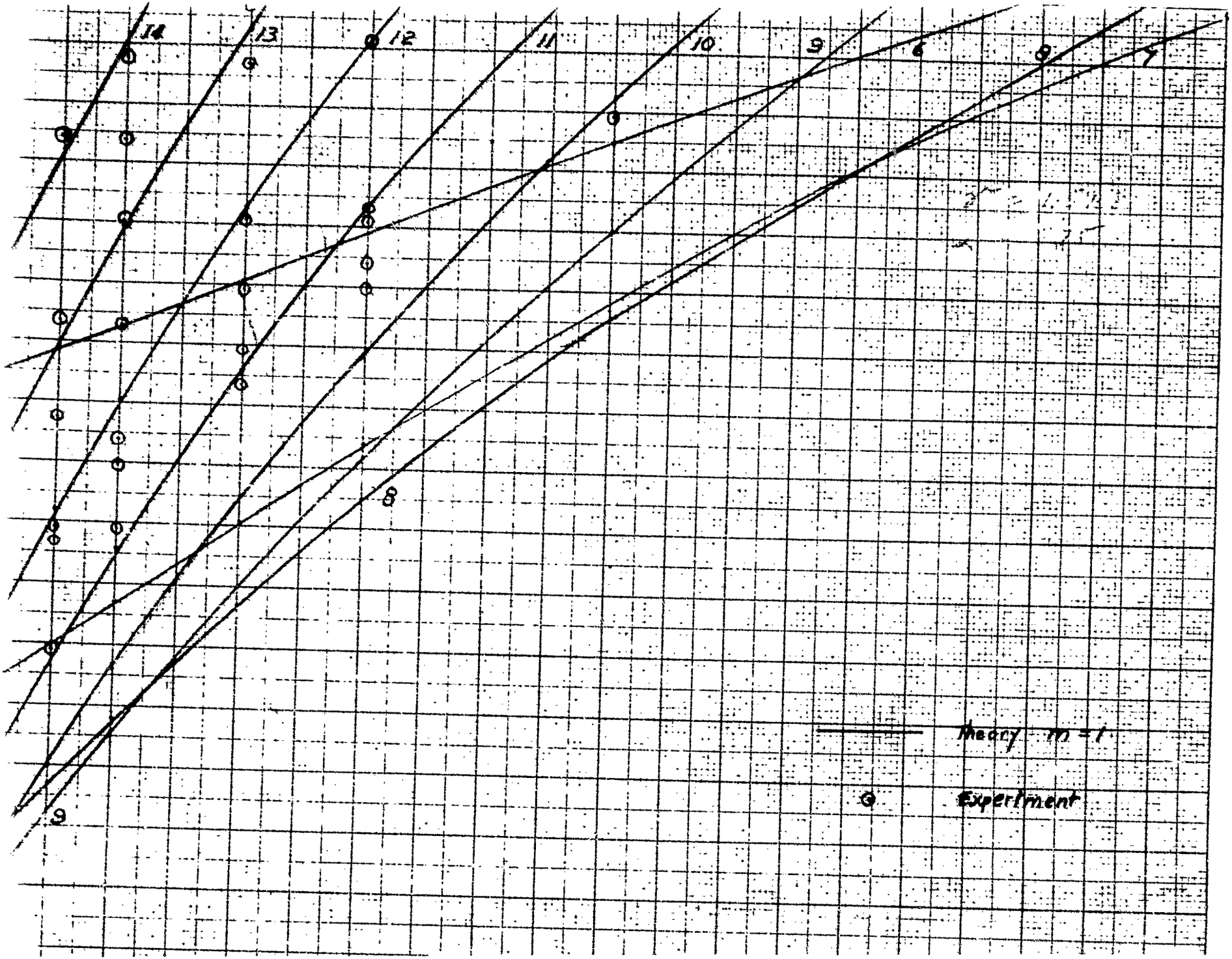
14
13
12
11
10
9
8
7
9
8
Theory m = 1
Experiment

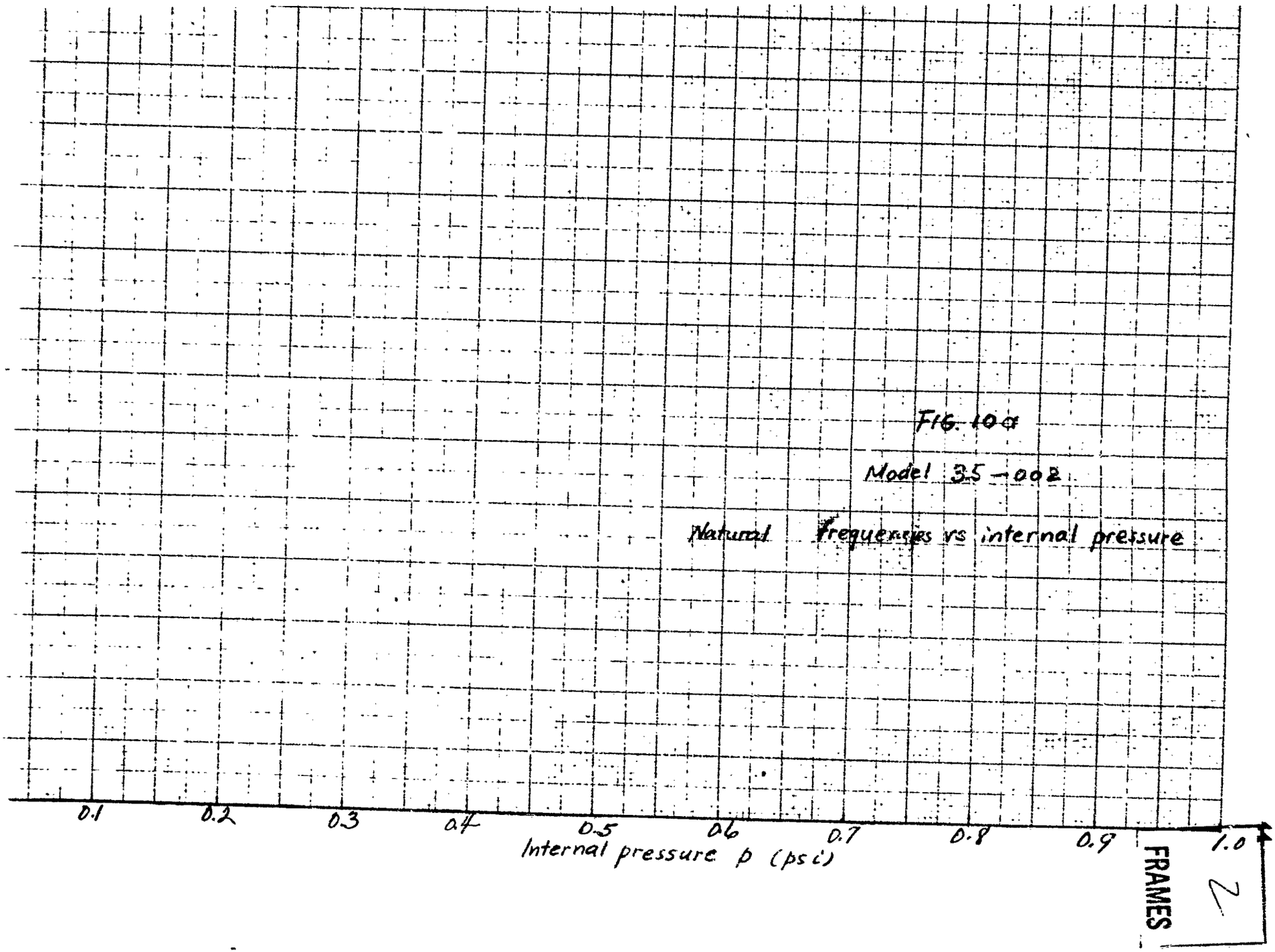

FIG. 10a

Model 35-002

Natural frequencies vs internal pressure

n=0
n=1
n=2
n=3
n=4
n=5
n=6
n=7
n=8
n=9
n=10
n=11
n=12
n=13
n=14
n=15
n=16
n=17
n=18
n=19
n=20

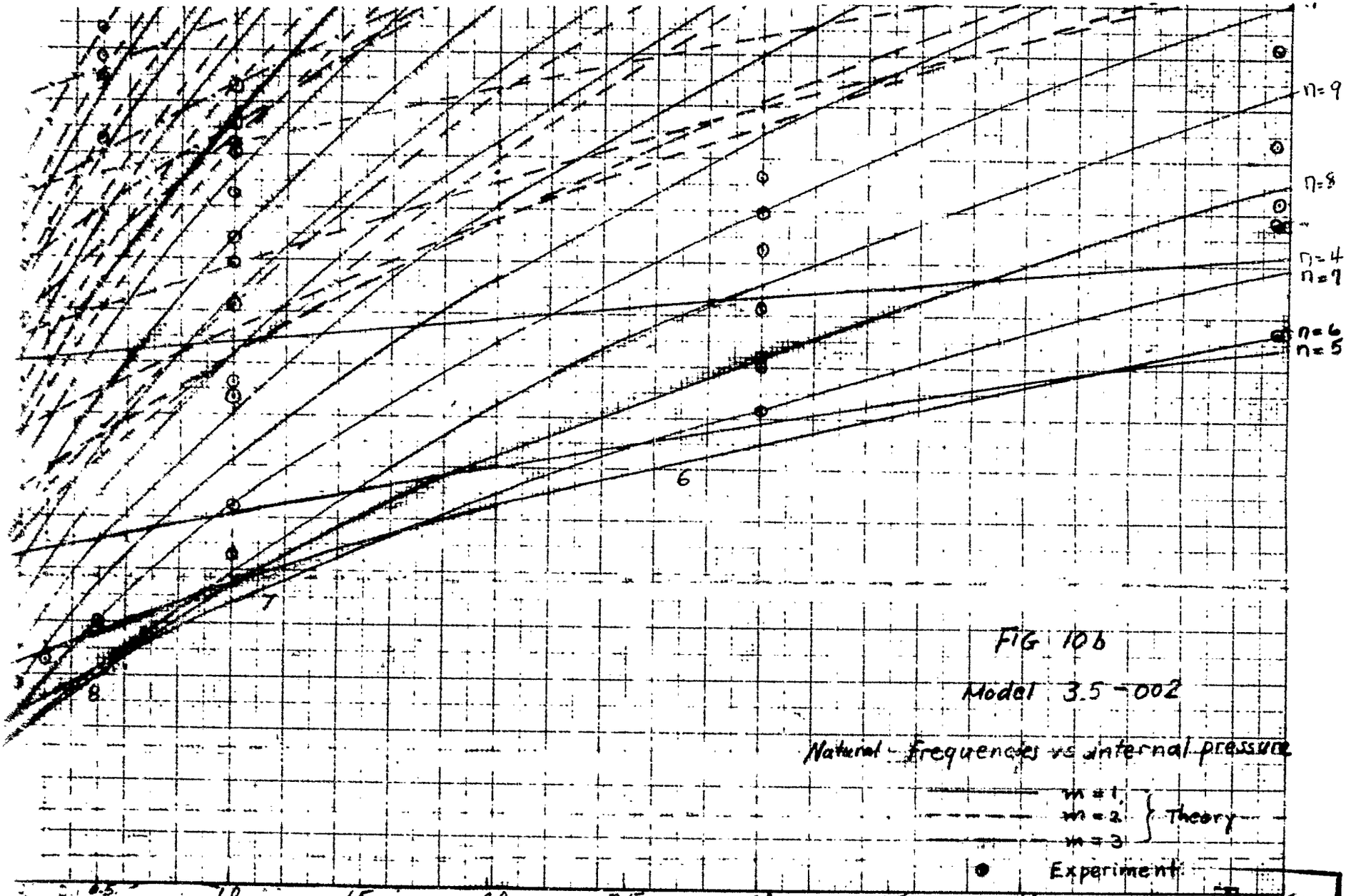
n=9
n=8
n=4
n=7
n=6
n=5
6
7
8
0.5
1.0
1.5
2.0
2.5
3.0
3.5
4.0
4.5
5.0
Internal pressure (psi)
P
FIG 10b
Model 3.5-002
Natural Frequencies vs internal pressure
m=1
m=2
m=3
Theory
Experiment
FRAMES
2

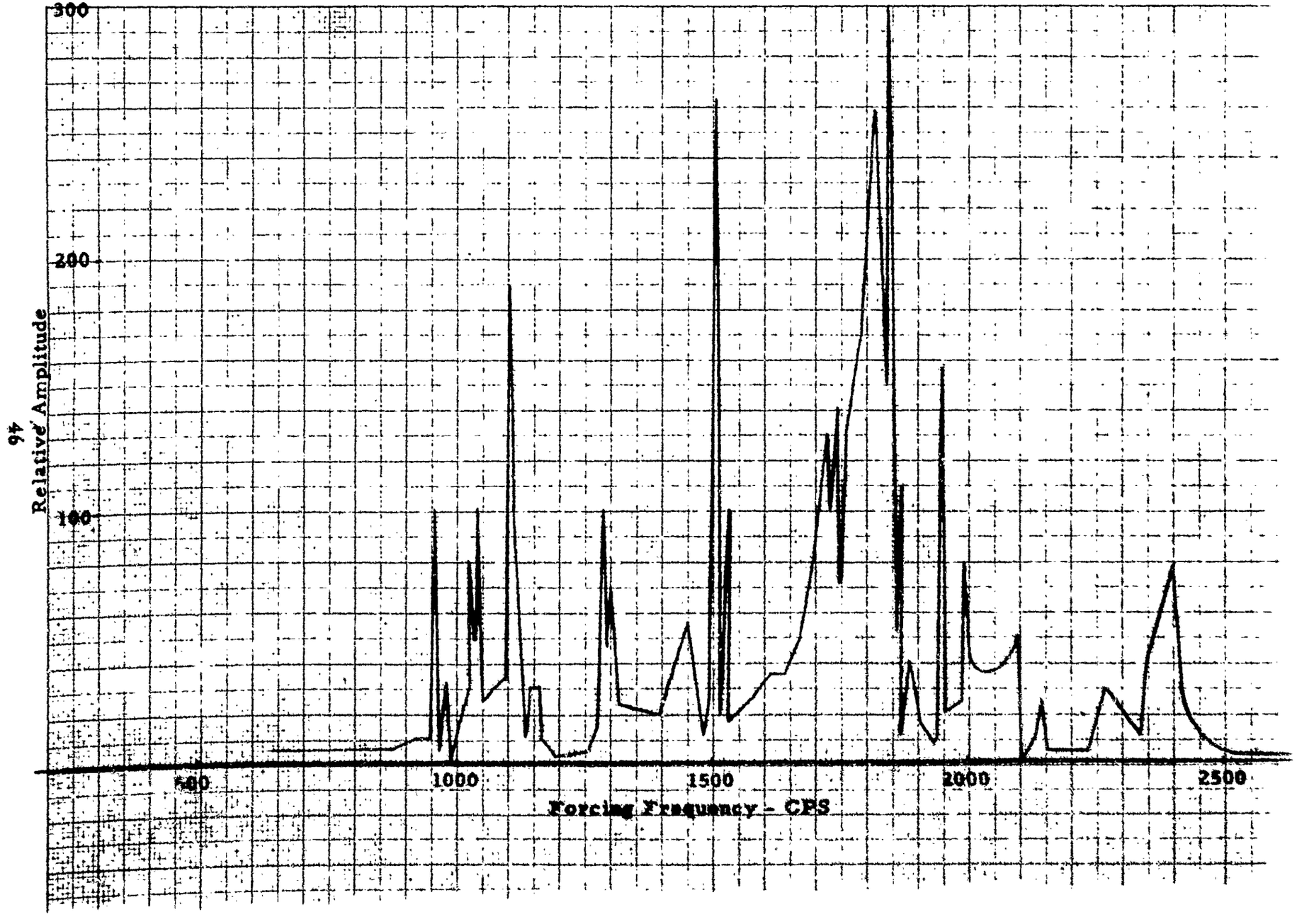

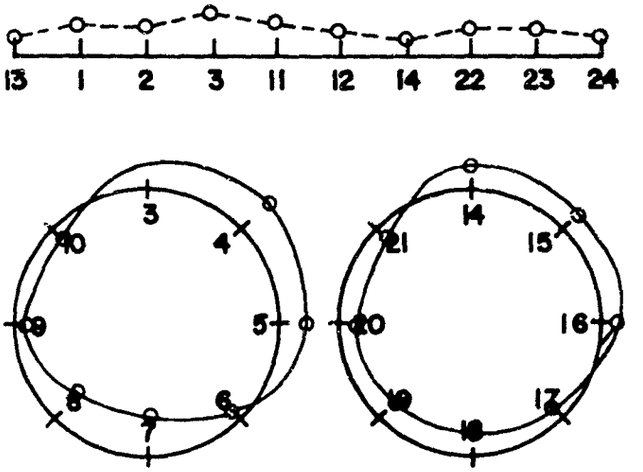

M=1, N=1

12(a). Record 12 11-001, f=550, p=0.1
Records 28(p=0.5), 35(p=3.5), 43(p=4.95) are identical

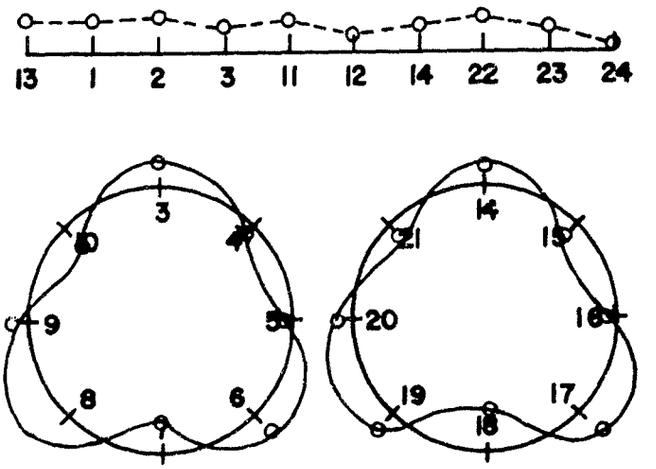

M=1, N=3

12(b). Record 29 11-001 f=763 p=0.50

Fig. 12. Mode Shape Determination

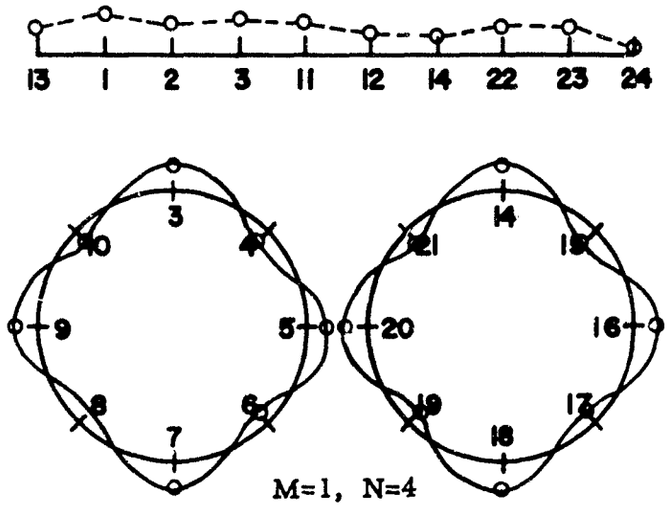

12(c) Record 37 11-001 f=1439 p=3.5

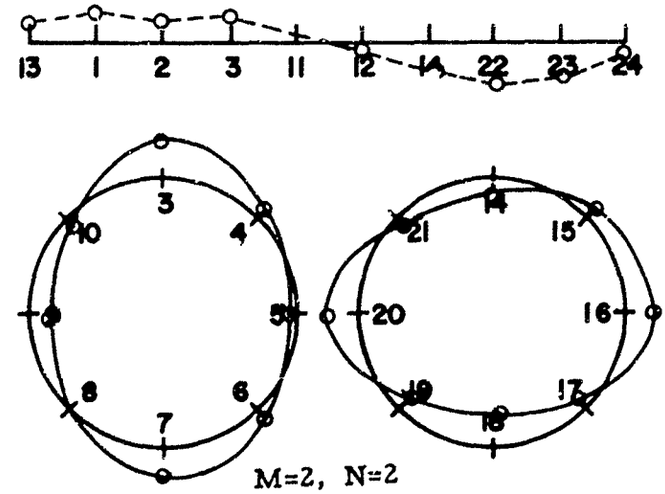

12(d), Record 40 11-001 f=2288 p=3.5

Fig. 12 Mode Shape Determination

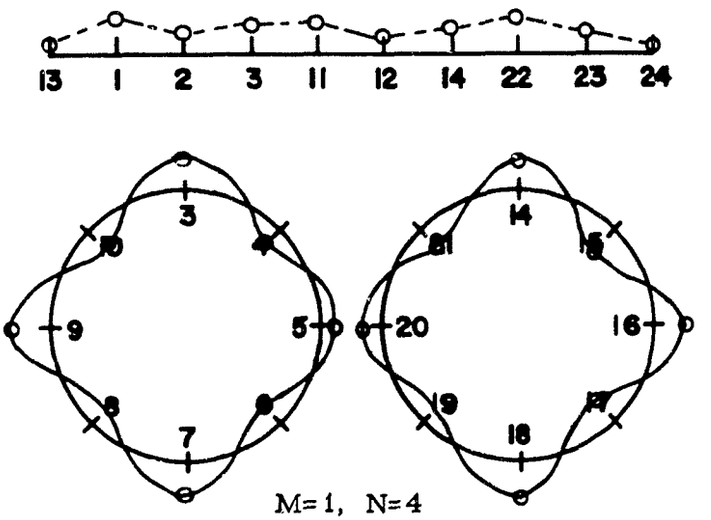

12(e) Record 44 11-001 f=1669 p=4.95

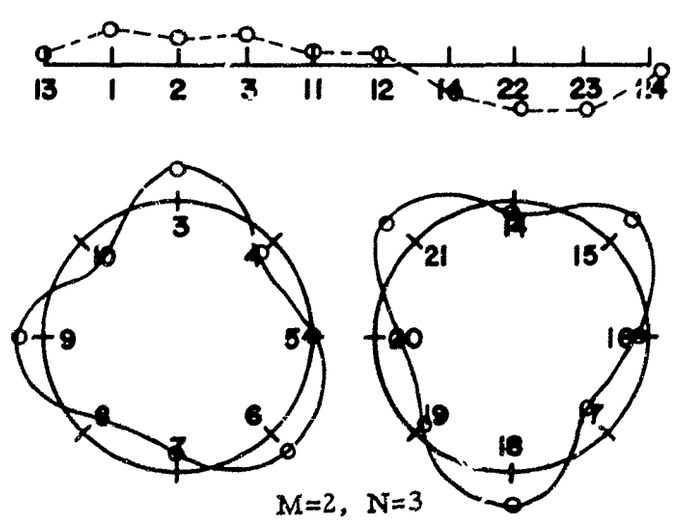

12(f) Record 45 11-001 f=2256 p=4.95

Fig. 12 (cont'd) Mode Shape Determination

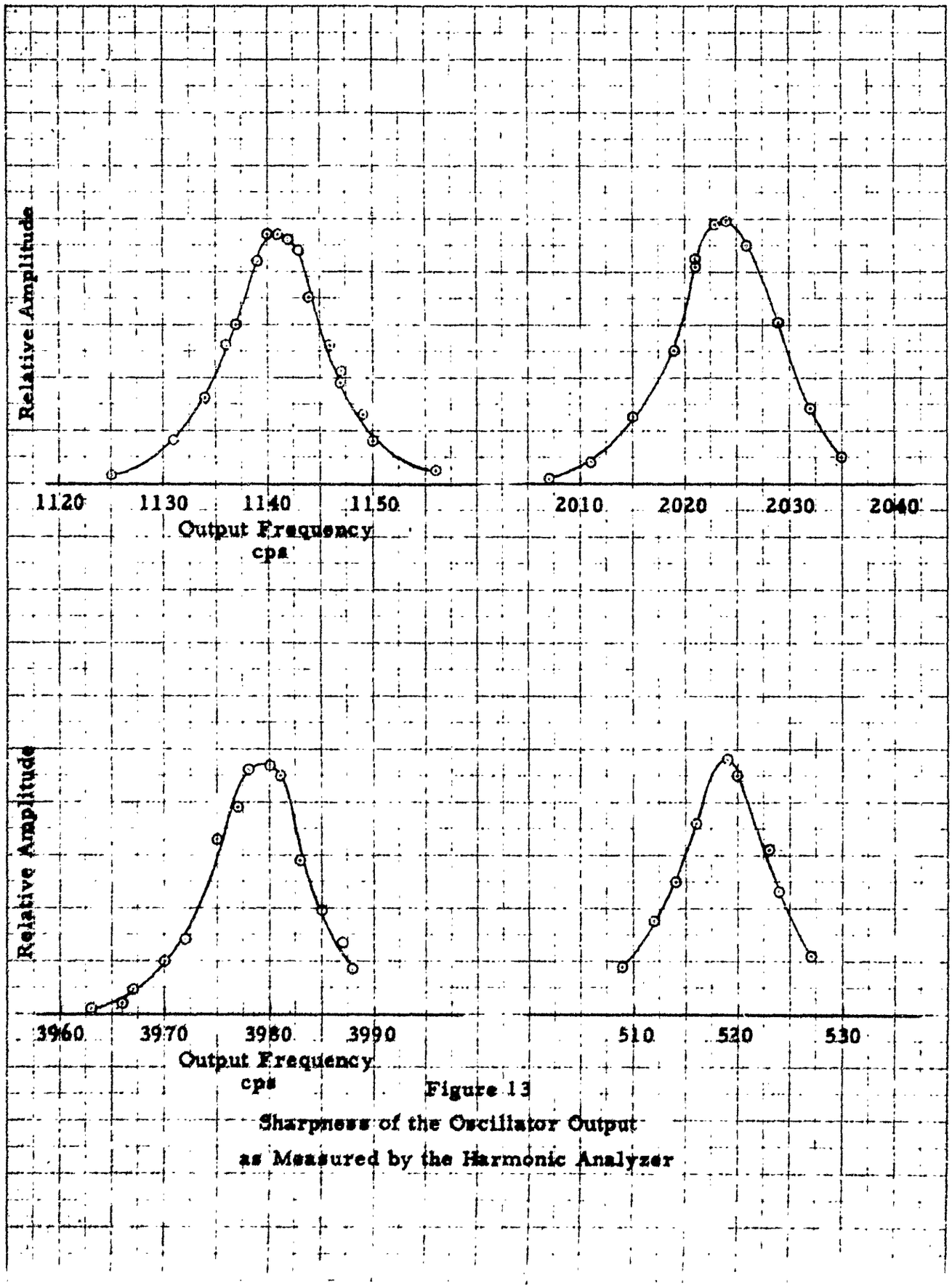

Figure 13

Sharpness of the Oscillator Output

as Measured by the Harmonic Analyzer

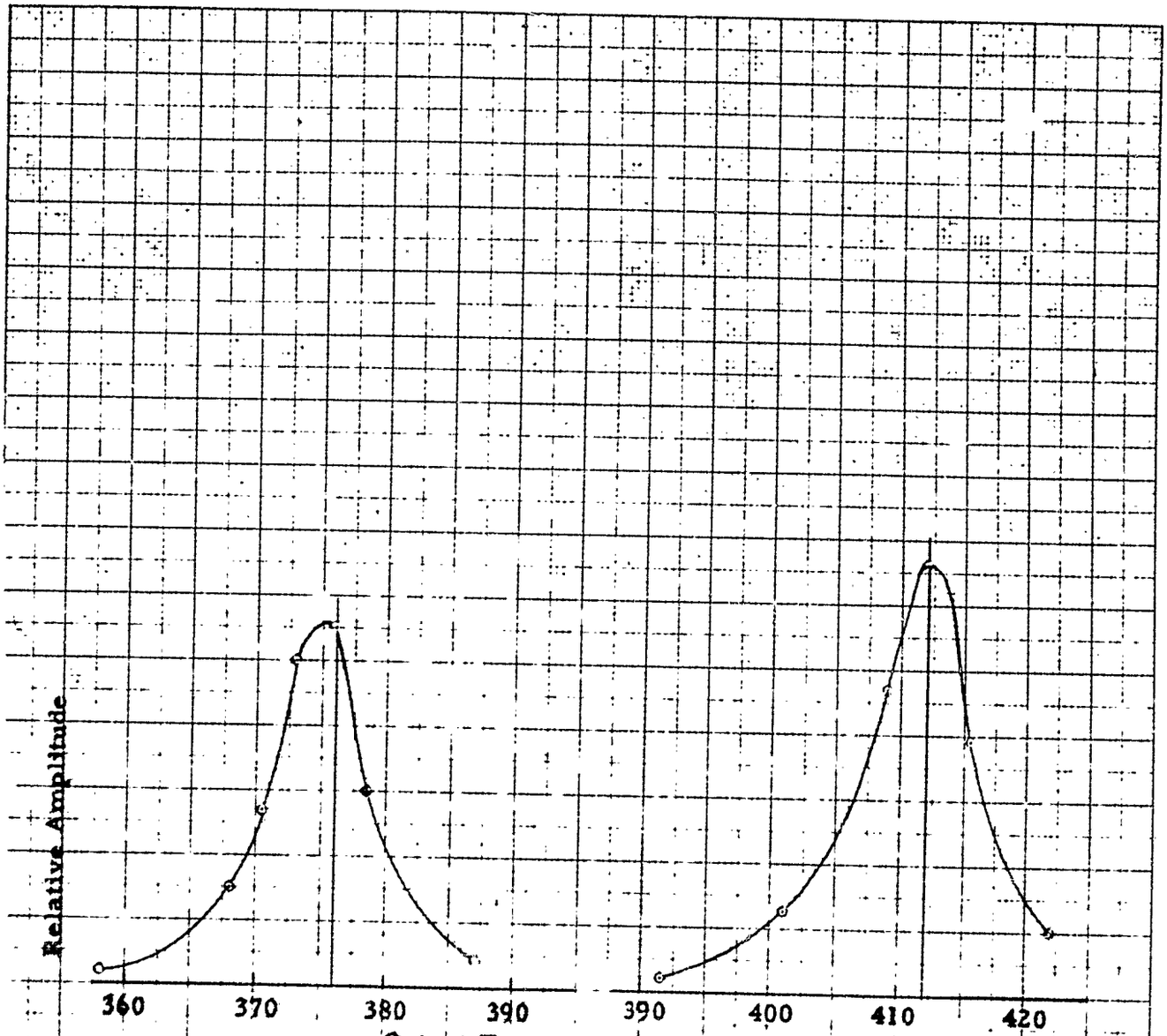

Figure 14

Sharpness of the Response of the 7-001 Cylinder at Specific Forcing Frequencies (p = 0.00)

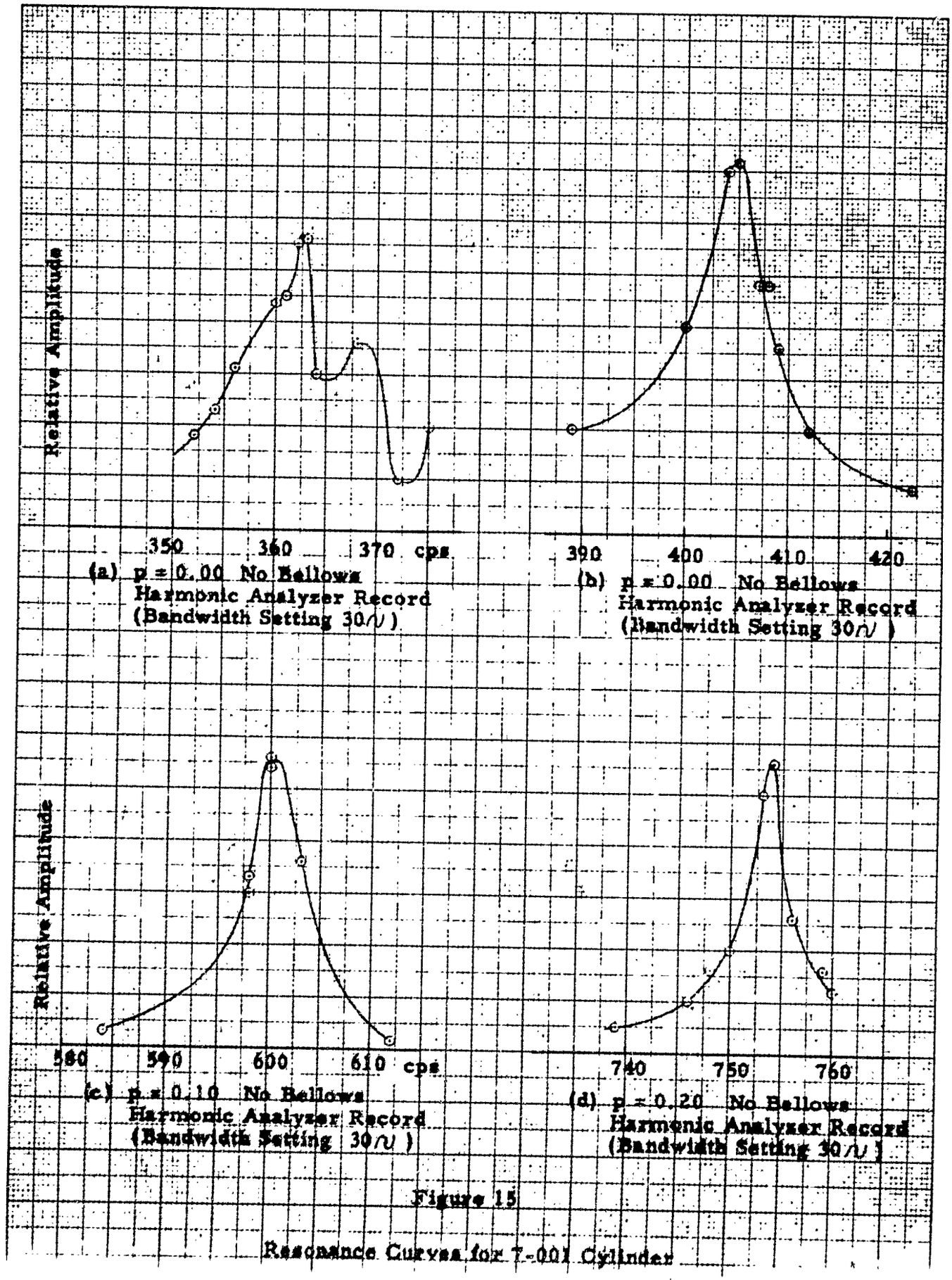

Figure 15

Resonance Curves for T-001 Cylinder

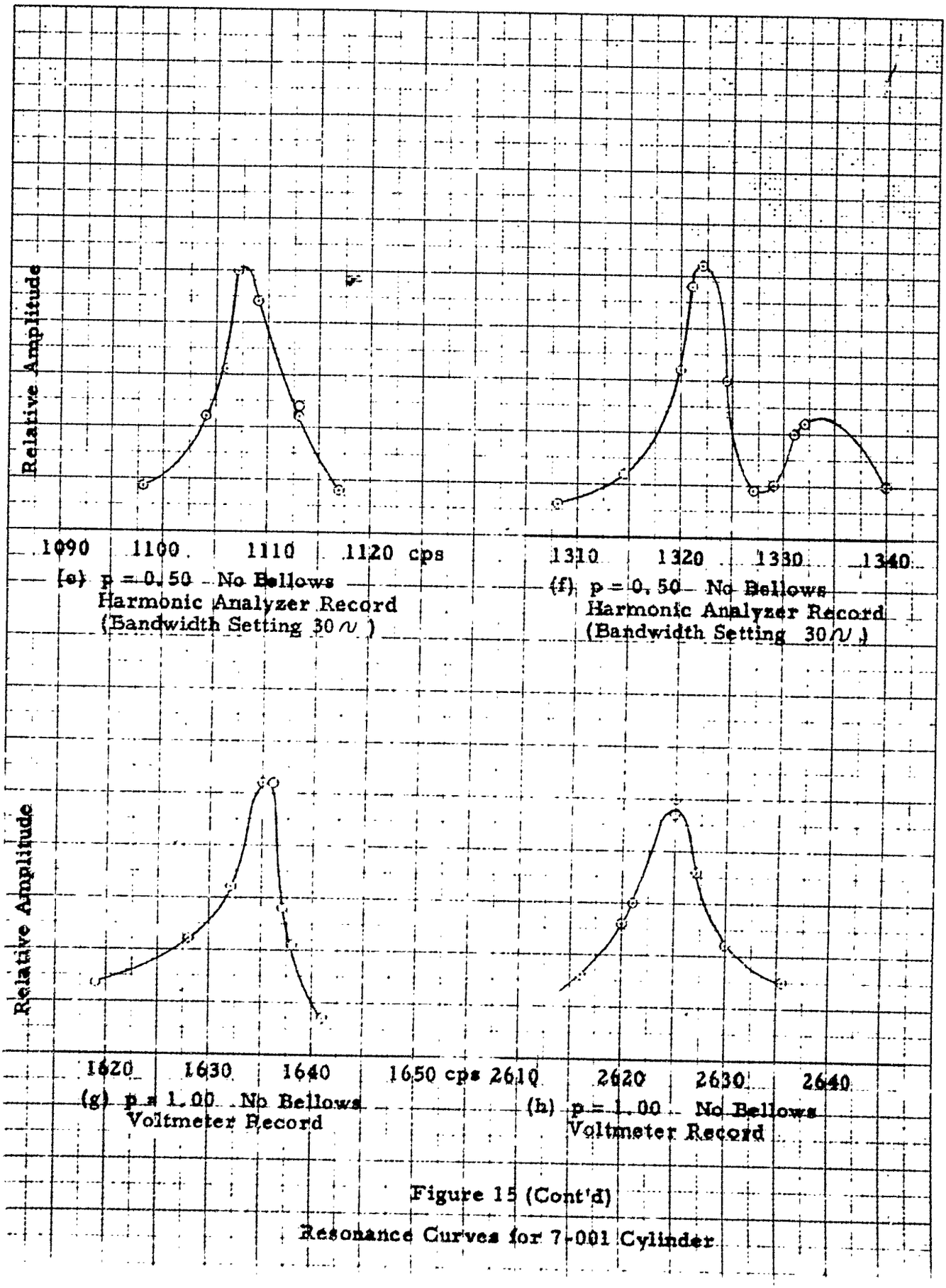

Figure 15 (Cont'd)

Resonance Curves for 7-001 Cylinder

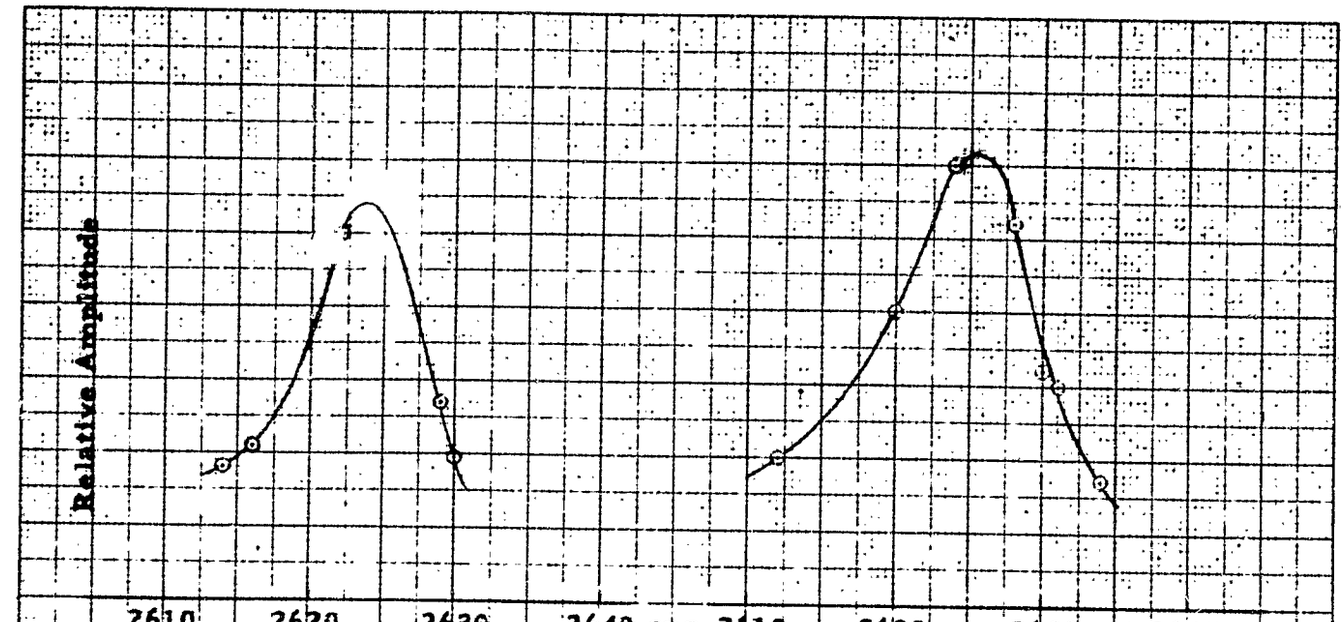

(i) p = 1.00 No Bellows
Harmonic Analyzer Record
(Bandwidth Setting 30 ∿)

(j) p = 1.00 No Bellows
Harmonic Analyzer Record
(Bandwidth Setting 145 ∿)

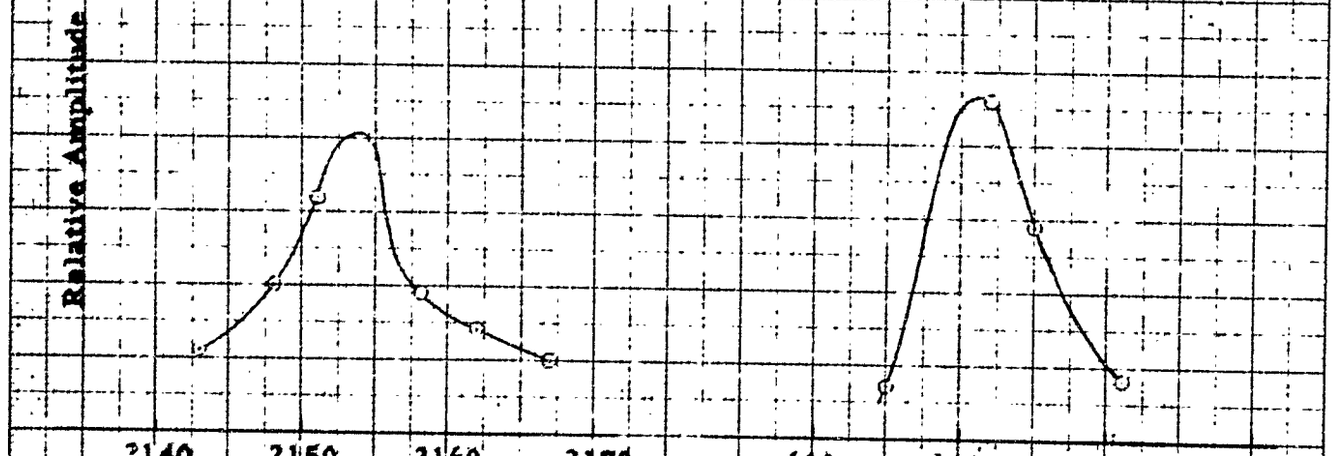

(k) p = 4.95 No Bellows
Harmonic Analyzer Record
(Bandwidth Setting 30 ∿)

(l) p = 0.10 No Bellows
Voltmeter Record

Figure 15 (Cont'd)

Resonance Curves for T-001 Cylinder

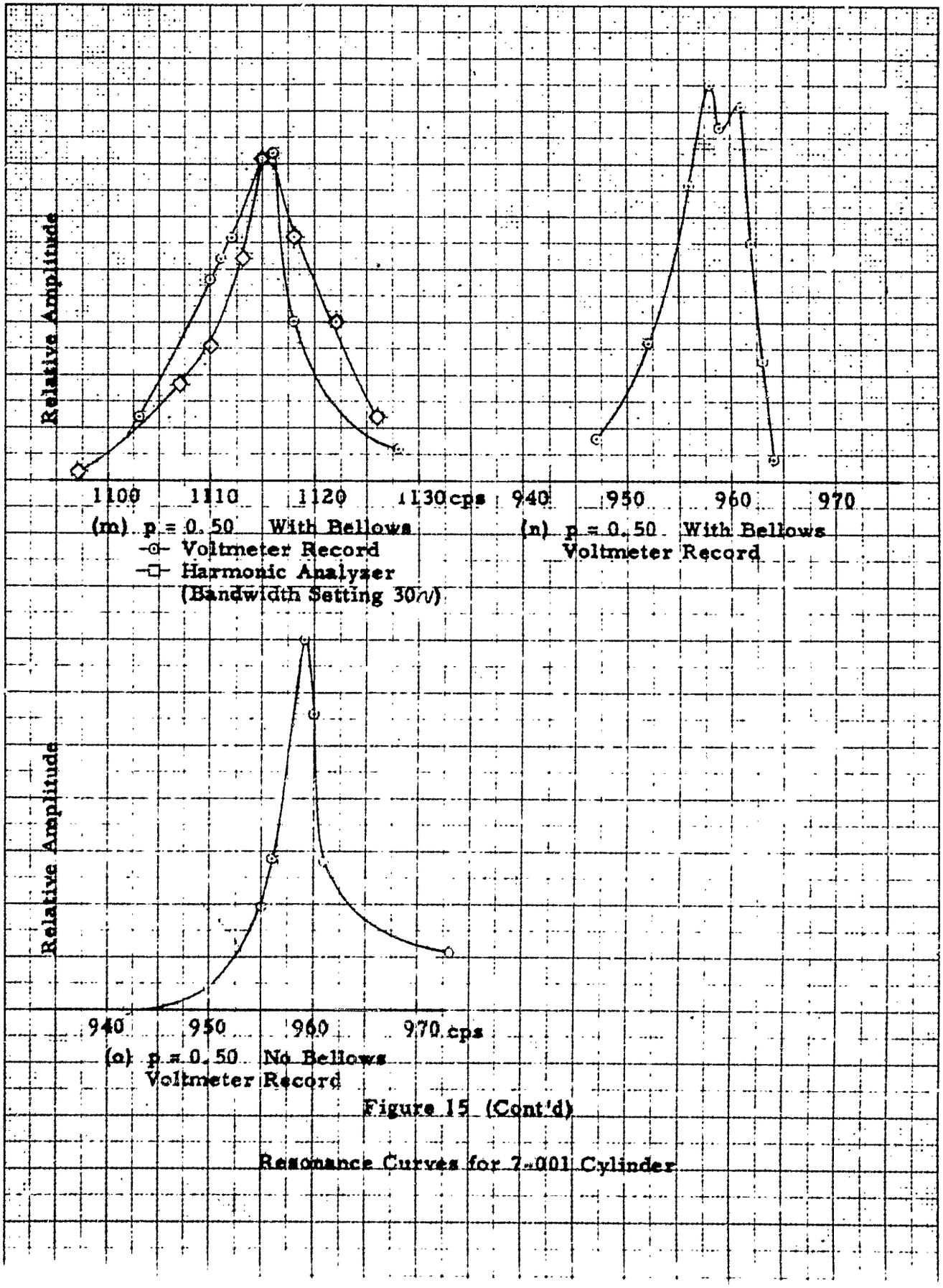

Figure 15 (Cont'd)

Resonance Curves for 7-001 Cylinder